

**Investigating Tup1-Cyc8 complex function in *Saccharomyces cerevisiae*
following the confirmation and characterization of a *TUP1* conditional
mutant**

**A dissertation presented for the degree of Master of Science, in the Faculty of Science,
University of Dublin, Trinity College**

2023

Pranay Agarwal

**Department of microbiology
Moyne institute of Preventative Medicine
Trinity College Dublin**

Declaration

I declare that this thesis has not been submitted as an exercise for a degree at this or any other university and it is entirely my own work.

I agree to deposit this thesis in the University's open access institutional repository or allow the library to do so on my behalf, subject to Irish Copyright Legislation and Trinity College Library conditions of use and acknowledgement.

I consent to the examiner retaining a copy of the thesis beyond the examining period, should they so wish (EU GDPR May 2018).

Abstract

The Tup1-Cyc8 complex is a well-defined corepressor complex found in *S. cerevisiae*. It is known to regulate close to 3% of all yeast genes and has orthologs reported in mammals. Its exact functioning is not well-understood. Here we use a conditional *TUP1* mutant of *S. cerevisiae* to perform time-course analysis of the events leading to Tup1-Cyc8 target gene derepression and assess the advantages of this mutant compared to a conventional *tup1* deletion mutant. To prepare the conditional mutant, the protein of interest (Tup1p) was first tagged with an FRB tag. The conditional mutants strain also contains the ribosomal protein RPL13A, fused with FKBP12, which binds to FRB in the presence of rapamycin. This leads to the FRB-tagged protein being ‘Anchored-away’ from the nucleus on the addition of rapamycin. The FRB tag was confirmed with a Western blot. The cells of the anchor-away strain acquired a flocculant phenotype at two hours post-rapamycin addition, a phenotype governed by the *FLO* family of genes. The *FLO1* gene was derepressed at 2 hours post-rapamycin addition and the *SUC2* gene at 40 minutes in the anchor away strains. *SEDI* was unaffected while *PMA1*, which is a housekeeping gene, maintained a stable transcription in all the strains. A ChIP assay following the Tup1p anchor away (Tup1-AA) time course showed that RNA Polymerase II levels correlated well with the transcription in the *FLO1* and *SUC2* genes. To study the occupancy of Cyc8p in the Tup1-AA strain, a modified Tup1-AA strain containing a 9-myc tagged Cyc8p (Cyc8-myc) was used, since a ChIP grade antibody for Cyc8p was unavailable. At the *FLO1* promoter following Tup1-AA, Tup1p levels declined while the detection of Cyc8-myc increased with time. However, Tup1p and Cyc8-myc were not detected at the repressed *SUC2* promoter, suggesting that the epitopes of both proteins may have been masked by the presence of other factors at this gene. Together, the Tup1-AA strain revealed that although Tup1p is lost from the *FLO1*

promoter following Tup1p anchor-away, Cyc8p persists where it could contribute independently to *FLO1* gene repression.

Acknowledgements

I would like to express my sincere gratitude to my supervisor, Dr. Alastair Fleming, for his unconditional support and mentorship during the project. I would like to thank my lab associates Brenda Lee and Reham Alnajjar for their support.

I would like to thank my postgraduate committee members Dr. Carsten Kröger and Dr. Siobhan O'Brien for their advice. I would also like to thank my colleagues at the Moyne institute for always being approachable and kind.

Table of Contents

Chapter 1

| | |
|--|----|
| Introduction | 11 |
| 1.1. Overview | 12 |
| 1.2. The eukaryotic chromosome | 13 |
| 1.3. Chromatin remodelling..... | 15 |
| 1.4. Post-translational modifications (PTMs) of histones | 17 |
| 1.5. The Tup1-Cyc8 complex | 20 |
| 1.6. The Anchor-away technique..... | 24 |

Chapter 2

| | |
|--|----|
| Materials and Methods | 28 |
| 2.1. Strains and growth parameters | 29 |
| 2.2. Protein extraction..... | 29 |
| 2.3. Total protein quantitation..... | 30 |
| 2.4. RNA extraction | 30 |
| 2.5. RNA visualization under denaturing conditions on an agarose- formaldehyde gel..... | 32 |
| 2.6. DNase treatment and cDNA generation | 33 |
| 2.7. Real-time qPCR..... | 34 |
| 2.8. Sodium Dodecyl Sulphate - Polyacrylamide gel electrophoresis (SDS- PAGE)..... | 35 |
| 2.9. Western Blotting | 36 |

| | | |
|------------------|---|-----------|
| 2.10. | Chromatin Immunoprecipitation (ChIP)..... | 37 |
| 2.10.1. | Cell growth and cross-linking..... | 37 |
| 2.10.2. | Preparation of cell lysates | 38 |
| 2.10.3. | DNA fragment size estimation..... | 39 |
| 2.10.4. | Immunoprecipitation (IP)..... | 39 |
| Chapter 3 | | |
| | Preliminary data | 42 |
| Chapter 4 | | |
| | Characterization of the Anchor-away strains | 45 |
| 4.1. | Introduction..... | 46 |
| 4.2. | Confirmation of the FRB tag | 46 |
| 4.3. | Visualizing the flocculant phenotype in Tup1-AA and Cyc8-AA cells following rapamycin addition..... | 48 |
| Chapter 5 | | |
| | Investigating the role of the Tup1-Cyc8 complex in gene transcription | 51 |
| 5.1. | Examining <i>FLO1</i> transcription in Tup1-AA and Cyc8-AA strains | 52 |
| 5.2. | Examining <i>SUC2</i> transcription in Tup1-AA and Cyc8-AA strains | 54 |
| 5.3. | Examining <i>SUC2</i> transcription in Tup1-AA and Cyc8-AA strains over a finer time-course | 54 |
| 5.4. | Examining <i>SEDI</i> transcription in Tup1-AA and Cyc8-AA strains..... | 57 |
| 5.5. | <i>PMA1</i> transcription is not de-repressed in Cyc8-AA and Tup1-AA strains following rapamycin addition..... | 58 |
| 5.6. | Discussion | 60 |

Chapter 6

Investigating the RNA Pol II, Tup1p and Cyc8p occupancy in the Tup1AA

strain.....

63

| | | |
|--------|--|----|
| 6.1. | Introduction | 64 |
| 6.2. | Confirming the Cyc8-myc strain | 66 |
| 6.3. | Optimizing the ChIP protocol..... | 68 |
| 6.4. | RNA Pol II occupancy at Tup1-Cyc8 repressed genes following Tup1p and Cyc8p depletion. | 70 |
| 6.4.1. | RNA Pol II occupancy at the <i>FLO1</i> open reading frame | 71 |
| 6.4.2. | RNA Pol II occupancy at the <i>SUC2</i> open reading frame | 71 |
| 6.5. | Tup1p occupancy at the <i>FLO1</i> promoter in the Tup1-AA strain..... | 73 |
| 6.6. | Tup1p occupancy at <i>SUC2</i> in the Tup1-AA strain | 74 |
| 6.7. | Cyc8-Myc occupancy at <i>FLO1</i> promoter in the Tup1-AA strain..... | 77 |
| 6.8. | Cyc8-Myc occupancy at <i>SUC2</i> promoter in the Tup1-AA strain..... | 77 |
| 6.9. | Summary of Tup1p and Cyc8p ChIP data in the Tup1-AA strain | 78 |
| 6.10. | Discussion..... | 81 |
| | References | 84 |

List of Figures

| | |
|--|----|
| Figure 1. Levels of DNA packaging | 15 |
| Figure 2. Types of chromatin remodeller ATPases | 17 |
| Figure 3. A summary of some general histone PTMs..... | 19 |
| Figure 4. The proposed mechanisms underlying the functioning of the Tup1-Cyc8 complex | 24 |
| Figure 5. The Anchor-away technique | 27 |
| Figure 6. RNA visualization under denaturing conditions..... | 33 |
| Figure 7. The FLO1 and SUC2 transcription profiles in tup1 and cyc8 gene deletion mutants..... | 43 |
| Figure 8. Western Blot to detect the FRB tag on the AA strains..... | 47 |
| Figure 9. Observing flocculation over time | 50 |
| Figure 10. Flocculation control..... | 50 |
| Figure 11. <i>FLO1</i> expression measured using RT-qPCR in the anchor-away time-course..... | 53 |
| Figure 12. <i>SUC2</i> expression measured using RT-qPCR in the anchor-away time-course..... | 56 |
| Figure 13. <i>SUC2</i> expression measured using RT-qPCR in a finer anchor-away time-course . | 57 |
| Figure 14. <i>SED1</i> expression measured using RT-qPCR in the anchor-away time-course..... | 58 |
| Figure 15. <i>PMA1</i> expression measured using RT-qPCR in the anchor-away time-course..... | 59 |
| Figure 16. The ChIP assay | 65 |
| Figure 17. Western blot to confirm the myc tagging in the Cyc8-myc strain..... | 67 |
| Figure 18. Confirmation of Cyc8p function in the Cyc8-myc..... | 68 |
| Figure 19. Sonication for chromatin fragmentation..... | 69 |
| Figure 20. Target controls and the normalization method for ChIP assays | 70 |
| Figure 21. ChIP analysis of RNA Pol II occupancy at the FLO1 open reading frame | 72 |
| Figure 22. ChIP analysis of RNA Pol II occupancy at the SUC2 open reading frame | 73 |

| | |
|---|----|
| Figure 23. ChIP analysis of Tup1p occupancy at the FLO1 promoter | 75 |
| Figure 24 ChIP analysis of Tup1p occupancy at the SUC2 promoter | 76 |
| Figure 25. ChIP analysis of Cyc8-myc occupancy at the FLO1 promoter..... | 79 |
| Figure 26. ChIP analysis of Cyc8-myc occupancy at the SUC2 promoter | 80 |

List of Tables

| | |
|---|----|
| Table 1 Oligonucleotides used in this study..... | 35 |
| Table 2 Primary antibodies used in the western blots..... | 37 |
| Table 3 Antibodies used in ChIP..... | 41 |

Chapter 1

Introduction

1.1. Overview

Saccharomyces cerevisiae has proved an ideal model organism to understand the functioning of genes and proteins under a variety of environmental conditions. Its permissivity to genetic manipulation and its genome being fully sequenced are major contributors responsible for this feature (Botstein and Fink 2011).

Characteristic of eukaryotes, the genome in *S. cerevisiae* exists in a highly compact form. The fundamental subunit of the DNA-protein complex which packages the genome is called the nucleosome. A single nucleosome particle has 147 base pairs of DNA wrapped around a histone octamer comprising two each of the core histone proteins, H2A, H2B, H3 and H4. These nucleosomes are further packaged together by linker histones to generate the complex chromatin. This compaction ensures that the ~12 Mb of the genome fits into the nucleus of *S. cerevisiae*. However, the DNA remains accessible for routine cellular processes like replication, transcription, and damage repair. This accessibility is regulated by numerous post-translational modifications, such as histone acetylation, and chromatin remodeling complexes like SWI-SNF and ISWI which function via their ATP-dependent helicase activity (Smith and Peterson 2004).

In contrast to factors making the genome more accessible, the Tup1-Cyc8 is a co-repressor complex that was the first transcriptional co-repressor described in *S. cerevisiae* (Wong and Struhl 2011a). It is composed of one Cyc8 (107 KDa) and four Tup1 subunits (80 KDa) (Varanasi et al. 1996). It is known to repress 300-500 different yeast genes (~6% of all *S. cerevisiae* genes) (Parnell et al. 2021). The Tup1 protein (Tup1p) is highly conserved in Fungi and has a well-described homolog in mammals known as the transducing-like enhancer of split (TLE). It does not possess intrinsic DNA-binding ability and is recruited

to the target promoter sites by interacting with DNA-binding transcription factors (Payankaulam et al. 2010). The mechanisms to explain its function include; (i) inhibition of the recruitment of RNA Polymerase II (RNAP II), the enzyme which catalyzes the transcription of DNA to mRNA (Papamichos-Chronakis et al. 2000); (ii) recruitment of histone deacetylases to the promoter region of genes (Fleming et al. 2014), (iii) preventing the recruitment of transcription activators to promoters (Wong and Struhl 2011a), and (iv) increasing the nucleosome occupancy in the promoter region of target genes to block initiation of transcription (Zhang and Reese 2004).

A well-documented function of the Tup1-Cyc8 complex is the repression of the *FLO1* gene (Church et al. 2017). *FLO1* is one of a family of genes responsible for controlling flocculation in the wild-type *S. cerevisiae*, by encoding a cell surface protein which forms lectin-like linkages with the cell wall components of surrounding yeast cells (Govender et al. 2008), (Smukalla et al. 2008). Tup1-Cyc8 is independently capable of controlling flocculation and deletion of either *TUP1* or *CYC8* leads to a strong flocculant phenotype (Teunissen et al. 1995).

1.2. The eukaryotic chromosome

The chromosome is the most compact form of eukaryotic DNA (Fig.1). It is comprised of a single molecule of DNA along with several proteins. In a diploid animal cell, the sister chromatids are conjugated with each other at the centromere (Rando and Winston 2012). There also exists at the ends of the chromosome, a telomere. It is a region of the chromosome that protects it from fusing with other chromosomes and being recognized as a site of DNA damage (Jafri et al. 2016).

The next highest level of compaction is chromatin. It is a fibrous complex composed of DNA and associated proteins, including a high abundance of histones. Histones are proteins which form a core for the DNA to wrap around. Rich in basic amino acids lysine and arginine, they are greatly suited to bind to negatively charged DNA. The histone structure can be subdivided into globular domains, which make up the nucleosome and the N- and C-terminal tails that protrude from the globular domain in the nucleosome (Tropberger and Schneider 2010). There are five different types of histones; histone H1 (linker histone), and the core histones, H2A, H2B, H3 and H4 (core histones). The linker histone H1 is associated with its role as a transcriptional repressor. Apart from contributing steric hindrance to the chromatosomes, it also inhibits remodeling by several ATP-dependent complexes (Brown 2011). A host of other non-histone proteins are also present in chromatin, which serve roles in gene expression and DNA replication. In an interphase cell, chromatin can be observed in two forms – euchromatin and heterochromatin. Euchromatin is less compact and hence, transcriptionally permissive while heterochromatin exists in a highly condensed state and is restrictive to transcription (Cooper 2000).

The repeating structural unit of chromatin is the nucleosome (Figure 1). Each nucleosome core particle contains 146 base pairs of DNA wrapped 1.65 times around a histone octamer. One molecule of the linker histone H1 is present, bound to the DNA as it enters the nucleosome core particle. This together forms a chromatin subunit called the chromatosome. These chromatosomes are separated by linker DNA to form a ‘beads on a string’ structure of the chromatin (Cooper 2000).

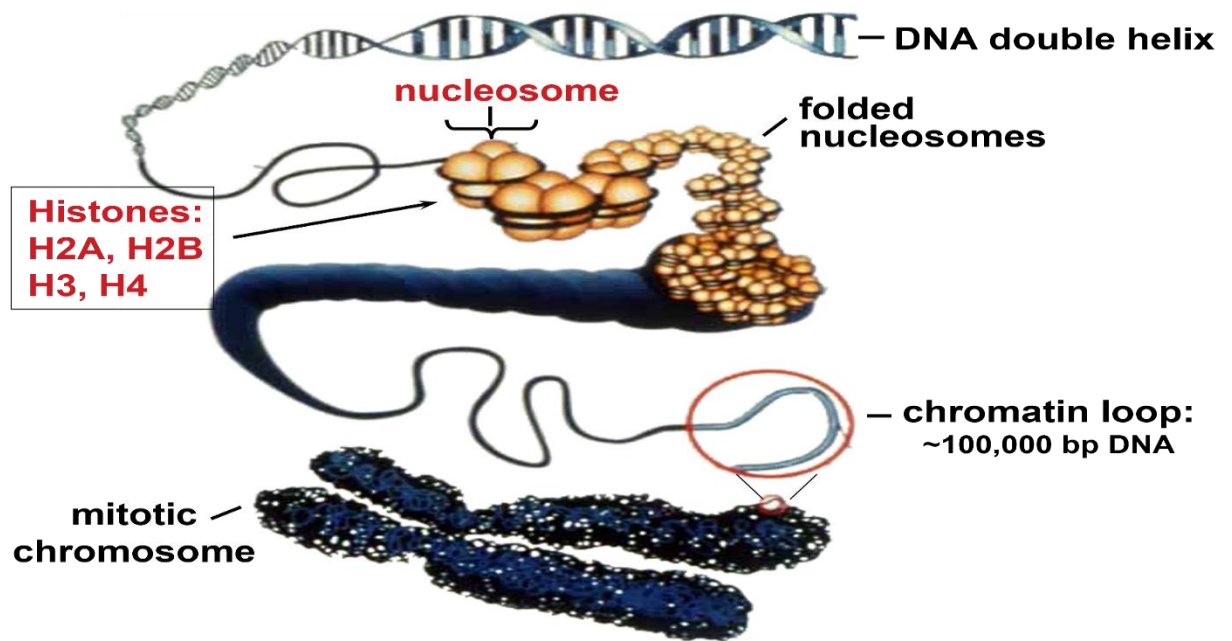


Figure 1. Levels of DNA packaging. Naked DNA wraps around the histone particles to form nucleosomes, which are linked by linker DNA to form the beads on a string structure, which lay the foundation for the chromatin and ultimately, the chromosome. Picture taken from (Luo et al. 2011)

1.3. Chromatin remodelling

Chromatin in its condensed form is generally impermeable to gene expression. It undergoes remodelling via several mechanisms to assume a more ‘open’ structure, allowing gene expression and DNA replication. This remodelling is carried out by chromatin remodellers, all of which contain an ATPase domain. They utilize energy from ATP hydrolysis to mobilize and reposition DNA along the histone surface. These ATPase complexes are characterized by the presence of two Rec-A like lobes, which ‘hold on’ to the DNA through a DNA-binding cleft and a site for ATP binding and hydrolysis. These together make up the DNA translocation motor. These Rec-A like lobes now advance along a single DNA strand, releasing 1-2 bp of DNA per cycle of ATP binding-hydrolysis-release. In terms of nucleosomes, a translocation of ~10 bp causes 1 helical rotation of DNA.

These remodellers are classified into four subfamilies: ISWI (Imitation switch), CHD (Chromodomain helicase DNA-binding), SWI/SNF (switch/sucrose non-fermentable) and INO80 (INOsitol requiring) (Clapier et al. 2017a) (Fig. 2).

The ISWI and the CHD subfamilies facilitate the development of mature octameric canonical nucleosomes from the initial nascent DNA-histone complexes followed by the bi-directional sliding of nucleosomes along the DNA to assemble them in a way to restrict gene accessibility. In the ISWI subfamily, the two Rec-A like lobes separated by an insertion sequence; and a carboxy-terminal HSS (HAND-SANT-SLIDE) domain together comprise the ATPase domain. The ATPase domains are flanked by the AutoN (autoinhibitory N terminal) and the NegC (negative regulator of coupling) domains, which regulate their activity. The CHD subfamily bears an ATPase domain largely like ISWI but also bears two tandemly arranged chromodomains on its N-terminal. Concerning *S. cerevisiae*, the ISWI subfamily comprises ISW1a, ISW1b and ISW2 while the CHD subfamily is monomeric (Clapier et al. 2017b).

The SWI/SNF subfamily can function to alleviate or repress DNA expression by destabilizing the histone octamer leading to nucleosome ejection or by sliding nucleosomes. Their ATPase domain is constituted by the two Rec-A like lobes, an N-terminal HSA (helicase/SANT-associated) domain, a post-HAS domain, AT-hooks and a C-terminal bromodomain. The SWI/SNF subfamily in yeast is composed of the Swi2/Snf2 ATPases (Clapier et al. 2017b).

The INO80 subfamily comprises Ino80p and Swr1p ATPases. Divergent from the other remodeller subfamilies, the INO80's ATPase domains are split by a spacer region, which is

essential to the maintenance of its overall structure. They also contain RuvB-like proteins, which are essential for the organism's growth and survival (Morrison and Shen 2009).

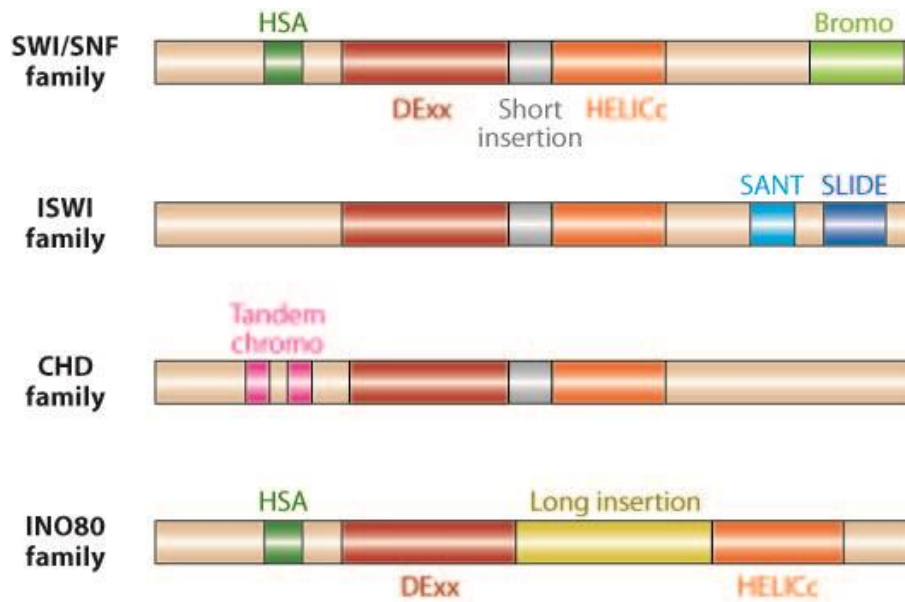


Figure 2. Types of chromatin remodeller ATPases. The ISWI (Imitation switch) and CHD (Chromodomain helicase DNA-binding) families are structurally and functionally similar to each other while the INO80 (INOsitol requiring) and SWI/SNF (switch/sucrose non-fermentable) possess a different structure and mechanism. Picture taken from Clapier and Cairns 2009.

1.4. Post-translational modifications (PTMs) of histones

Histone PTMs are covalent additions to the C-terminal and N-terminal of histone tails and in some cases, to the globular domain also. They are a key factor in regulating gene expression without modifications to the primary DNA sequence; a field referred to as epigenomics. Other mechanisms governing epigenetics are chromatin remodelling and the methylation of CpG islands of gene promoters (Ramazi et al. 2020), although this is not

known to be present in *Saccharomyces cerevisiae*. Some major categories of histone PTMs are described below and depicted in fig. 3.

Histone acetylation is the reversible transfer of an acetyl group from acetyl-CoA to the lysine residues on the histone N-terminals, catalyzed by enzymes called HATs (histone acetyltransferases). Acetylation of lysine neutralizes the positive charge on the unmodified side chains on lysine residues, thus weakening its interaction with the negatively charged DNA backbone, attenuating the overall histone-DNA interaction. Thus, these modifications have a key role in transcriptional activation (Tropberger and Schneider 2010). The enzymes that work to reverse acetylation are called HDACs (histone deacetylases), and they have a role in transcriptional repression. A significant subset of genes in yeast is regulated by the HATs Gcn5p and Rpd3p (Ramazi et al. 2020).

Histone phosphorylation is characterized by a reversible introduction of negatively charged phosphates to histones, which weakens their interaction with the negatively charged DNA backbone. Serine, threonine, and tyrosine residues are the well-known targets of phosphorylation, which is catalyzed by kinases. Phosphorylation of histone H3 is reported to be vital for cell-cycle progression and chromosome condensation during cell division (Ramazi et al. 2020).

Histone methylation is another reversible histone PTM. It involves mono-, di- or tri-methylation of lysine residues and mono- or di- methylation of arginine residues, catalyzed by HMTs (Histone methyltransferases). Unlike acetylation and phosphorylation, it does not involve altering the net charge of the modified residues. The outcomes of methylation depend on the site(s) and the degree of methylation. For example, the trimethylation of

H4K20 and H3K27 in higher eukaryotes is linked with gene silencing and heterochromatin formation while the trimethylation of H3K4 and H3K36, present in yeast, are associated with transcriptionally active chromatin (Cavalieri 2021).

Ubiquitylation as a PTM of histones involves the isopeptide linkage of a single ubiquitin molecule to target lysine groups, primarily in H2A and H2B histones. Contrary to poly-ubiquitylation, which prepares proteins for proteasome-mediated degradation, mono-ubiquitylation of histones is linked with DNA-damage response and transcriptional regulation. In the case of H2AK119, mono-ubiquitylation strengthens the association of linker histone H1 and stimulates the tri-methylation of H3K27, which eventually promotes gene silencing and chromatin compaction (Cavalieri 2021).

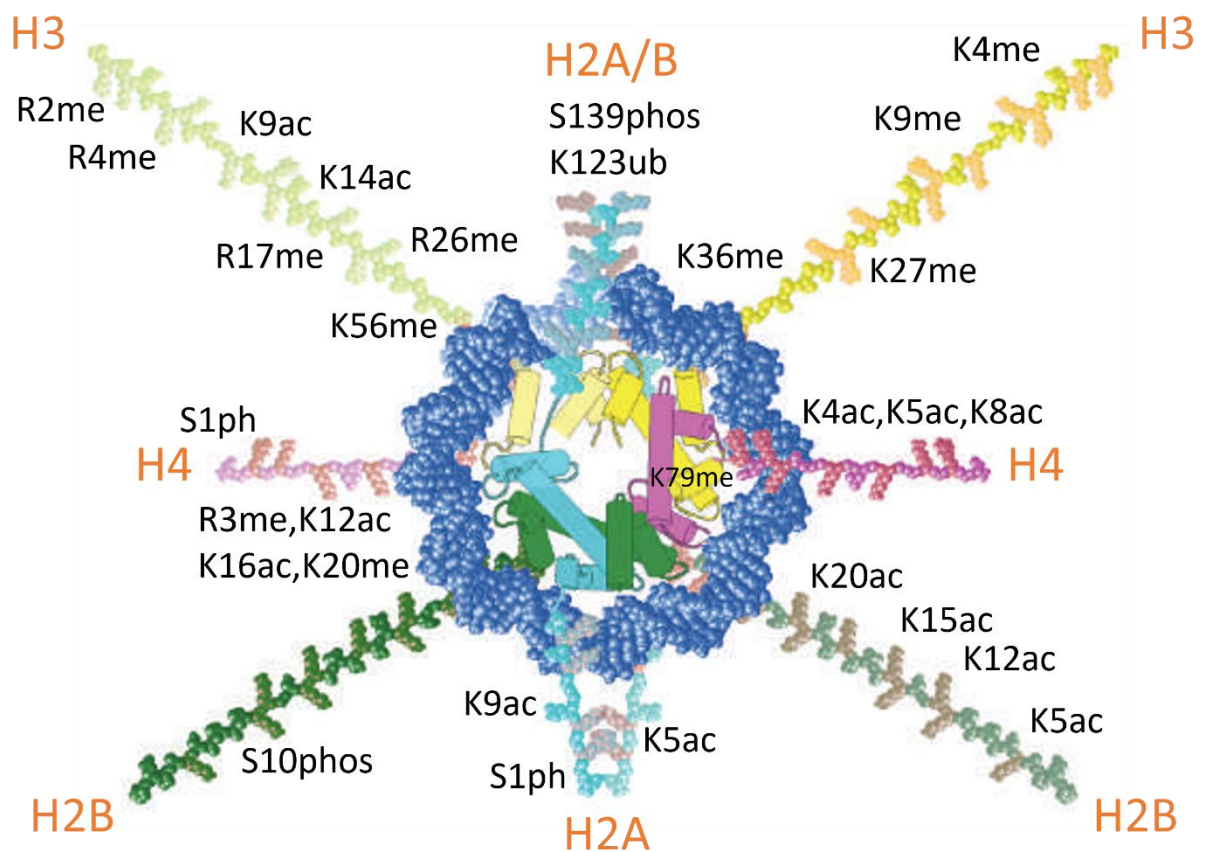


Figure 3. A summary of some general histone PTMs. Schematic to show examples of various histone PTMs including acetylation, phosphorylation, methylation and ubiquitylation of the core histone proteins indicated. Picture adapted from Kinner et al. 2008.

The phenomenon when these histone PTMs combine to orchestrate gene expression is called the ‘histone code’. The phosphorylation of H3 at Serine 10 (H3S10) is a classic example of this phenomenon. During interphase, phosphorylation of H3S10 is linked to the acetylation at H3K9 and H3K14, which leads to a more permeable chromatin structure for interaction with transcription factors. During mitosis, however, phosphorylation of H3S10 is associated with increased methylation at H3K9, resulting in chromatin condensation (Prakash and Fournier 2017). The factors catalyzing the various types of PTMs are classified as ‘writers’, ‘erasers’ and ‘readers’. Writers add PTMs to histones, erasers remove PTMs, and readers identify the PTMs and bring about the cellular outcome. A classic example of a reader is the bromodomain-containing subunit of Swi-Snf, Snf2p, which is vital for the full binding and activity of the SWI/SNF remodelling complex (Gillette and Hill 2015).

1.5. The Tup1-Cyc8 complex

The Tup1 protein (Tup1p) is composed of 713 amino acids and has a molecular mass of about 80 KDa. Its functional domain arises from sequences present in residues 120-334, as Tup1p fragments become non-functional upon the loss of this region. The C-terminal domain features seven WD40 repeats which assume the form of a 7-bladed propeller structure. These repeats are known to mediate protein-protein interactions. Residues 1-72 in the N-terminal domain feature sequences involved in its complex formation with Cyc8 (Jabet et al. 2000). Mutations in the *TUPI* (Thymidine uptake) gene have previously been isolated to investigate effects on phenotypes other than glucose repression. One of the first *tup1* mutants was isolated for their decreased ability to take up dTMP from the growth

medium and hence the name Tup1, which is short for Thymidine uptake, was coined (Williams et al. 1991).

Cyc8p, also known as Ssn6p (suppressor of *snf1*) is composed of 966 amino acids and weighs about 107 KDa. Residues 46-398 at the N-terminus contain a domain made up of 10 tetratricopeptide repeats (TPR), with each TPR made of 34 amino acids. These domains combine to carry out various functions of the protein. Motifs 1-3 are sufficient for direct binding with Tup1p; motifs 1-7 are required for the repression of O₂-regulated genes, and all the motifs are required for the repression of DNA damage-regulated genes (Jabet et al. 2000).

Tup1-Cyc8 has been described to function by several different mechanisms that are not mutually exclusive (Fig. 4). The first involves negatively influencing the general transcription machinery. Med6p is a holoenzyme component of RNA polymerase II that plays a role in the transmission of recruitment signals from transcriptional activators to RNA polymerase II and is thus involved in transcriptional activation. Srb7p is another holoenzyme component that has a role in transcriptional activation and repression. Both proteins are physiological targets of Tup1p, and Srb7p is a physiological target of Med6p. Med6p and Tup1p compete for binding with Srb7p. The Srb7p-Med6p binding is necessary for complete transcriptional activation by different activators. It was reported that replacing Srb7p with a mutant that is incapable of binding to Tup1p led to the de-repression of genes *MFA1*, *STE2*, *SUC2* and *GALI*, thus suggesting Tup1p-based repression by negatively influencing RNA polymerase II recruitment (Gromöller and Lehming 2000). The second proposed mechanism is that Tup1-Cyc8 interacts with histone deacetylases Rpd3p and Hda1p to remove acetyl groups from the N-terminal tails of

histones H2B, H3 and H4 and cause deacetylation of promoter histones to promote gene repression (Fleming et al. 2014). Histone tails are abundant in basic residues, arginine, and lysine. These are positively charged at a physiological pH and thus have a high affinity for negatively charged phosphate (PO^{3-}) groups on the DNA and thus promote chromatin compaction. Acetylation of the lysine residues hinders the interaction between DNA and the histone octamer, rendering chromatin more 'open' (Hong et al. 1993).

The third mechanism is that Tup1-Cyc8 may block the binding or the recruitment of transcriptional activators like Gcn5p and chromatin remodelling factors like SWI-SNF (Wong and Struhl 2011a). It has been reported that under de-repressing conditions (low glucose), the chromatin structure at the *SUC2* promoter in *snf2*, *snf5* and *swi1* (genes which transcribe components of the SWI-SNF complex) cells is identical to that in repressed (high-glucose) wild-type cells, suggesting the role of SWI-SNF in de-repression of *SUC2*. It was also observed that the chromatin structure disrupted in *tup1* and *cyc8* mutants under repressing conditions was restored in a *swi1* mutant. This is indicative of an antagonistic interaction between SWI/SNF and Tup1-Cyc8, where Tup1-Cyc8 may prevent the SWI/SNF from remodelling the chromatin (Gavin and Simpson 1997).

The fourth mechanism describes regulation by the ISWI (imitation switch) class of chromatin remodelling complex. Three ISWI complexes have been isolated from *S. cerevisiae*: ISW1a, ISW1b and ISW2. It was observed that deleting *ISW2* led to a complete disruption of nucleosome positioning via loss of nucleosome positioning upstream of the URS (upstream regulatory sequence) in *RNR3*. ISW2 functions via bi-directional sliding of nucleosomes along the DNA, Tup1-Cyc8 at the promoter region functions in synchronization with the ISW2 complex to regulate the positioning of nucleosomes to

adopt positions downstream of the URS and keep it from sliding nucleosomes upstream from the URS (Zhang and Reese 2004).

The *FLO1* gene is a well-studied gene proven to be under the transcriptional control of Tup1-Cyc8. It is part of the *FLO* family of genes that govern flocculation in yeast. They encode a cell surface protein which forms calcium-dependent lectin-like linkages with the carbohydrate residues of α -mannans in the cell walls of neighbouring yeast cells, leading to the formation of ‘flocs’ (Smukalla et al. 2008). The *FLO1* gene is independently capable of controlling flocculation. Other genes in the *FLO* family are *FLO5*, *FLO9*, *FLO10*, and *FLO11*. While *FLO1*, *FLO5*, *FLO9* and *FLO10* contribute to flocculation, *FLO11* is vital for cell-surface adhesions (Yang et al. 2018).

Another well-studied gene under Tup1-Cyc8 transcriptional control is the *SUC2* gene. It encodes for the enzyme invertase, which is required to utilize sucrose as a carbon source. It gets de-repressed in the absence of glucose in the growth medium (Vallier and Carlson 1991).

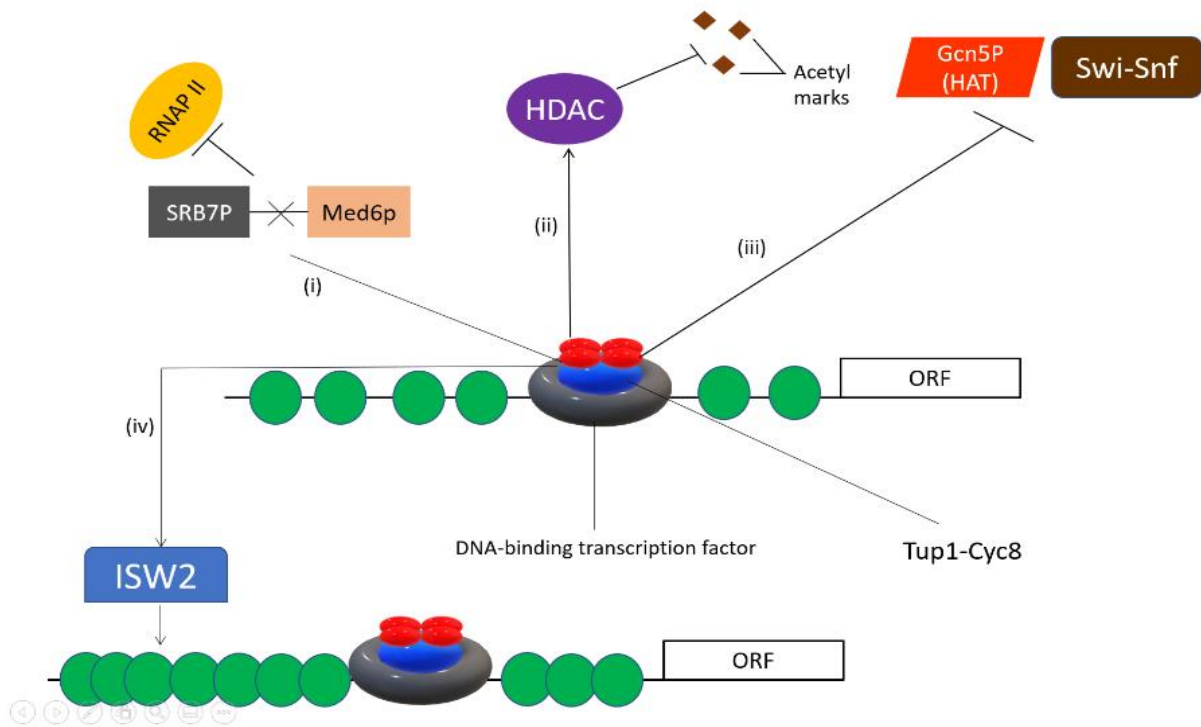


Figure 4. The proposed mechanisms underlying the functioning of the Tup1-Cyc8 complex. (i) Indirectly blocking RNAPII recruitment (ii) Recruitment of HDACs to the promoter site to confer a restrictive PTM (iii) Blocking the recruitment of Gcn5P and Swi-Snf complex (iv) Interacting with the NRC ISW2 to make the promoter region restrictive to transcription.

1.6. The Anchor-away technique

Haruki et al. devised a method that involves depleting the nucleus of a protein of interest (target) by binding it to a suitable receptor protein which serves as an ‘anchor’ (Haruki et al. 2008). The protein of interest was C-terminally fused with an 11 KDa FKBP12-rapamycin-binding (FRB) domain of the human mTOR (Mammalian Target of Rapamycin). The FRB-tagged protein of interest was now referred to as the target protein.

Several ribosomal proteins are known to traverse the nucleus during the assembly of the 40S and 60S ribosomal subunits (Zemp and Kutay 2007). This movement was utilized to transport the target protein out of the nucleus. The 60S ribosomal protein L13a (RPL13A)

was chosen as the anchor protein and was C-terminally fused with a human 12 kDa FK506 binding protein (FKBP12). If Rapamycin is added to the medium, it initially binds with the FKBP12 domain of the RPL13A-FKBP12 complex. This exposes a binding surface for the FRB domain on the FRB-tagged target protein to form a ternary complex with the anchor. This complex is shuttled out of the nucleus due to the movement of RPL13A. This mechanism is illustrated in fig. 5.

Haruki et al. observed that the RPL13A-FKBP12 *S. cerevisiae* strains grew robustly and as fast as the parental strains in both, the presence and absence of Rapamycin. It was effective in impeding the function of the FRB-tagged TATA-binding protein (TBP; *SPT15*). The Anchor-away technique serves several advantages over using the conventional deletion mutants. It allows for dynamic scrutiny of the events leading up to the nucleus being completely depleted of the gene product of interest, compared to a deletion mutant, which only reflects a snapshot of the endpoint. Deletion of the *CYC8* gene is reported to have a pleiotropic effect (a single gene affecting multiple characteristics in the phenotype) on the resultant strain. The anchor-away technique permits studying the occupancy of the RNAP II and the Tup1-Cyc8 proteins over time to better understand the mechanism of the events that occur at a gene during derepression.

Aim of the study

Most studies into Tup1-Cyc8 complex function have relied upon using *tup1* or *cyc8* gene deletion mutants. However, despite years of research, the precise mechanism of action of Tup1-Cyc8 is unknown. My project aimed to construct and characterize a *TUP1* conditional mutant. The rationale was that a conditional mutant of *TUP1* should be superior for study as compared to a *tup1* gene deletion mutant which might be subject to broad secondary effects. It was therefore hoped that a *TUP1* conditional mutant might allow for a more detailed and insightful analysis of Tup1-Cyc8 function at target genes. The Tup1-AA strain would allow a time course analysis following the de-repression of the Tup1-Cyc8 repressed genes, *FLO1* and *SUC2*.

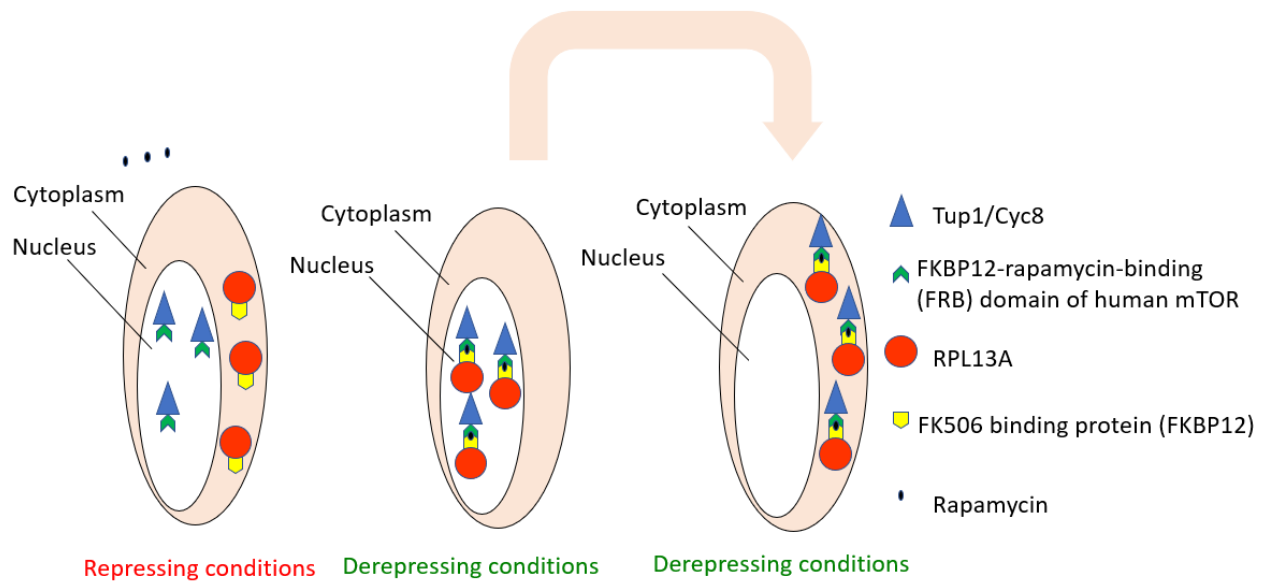


Figure 5 The Anchor-away technique

The protein of interest (Tup1 or Cyc8) is fused with an FRB tag. The presence of Rapamycin in the medium induces the formation of a ternary complex when the anchor protein (RPL13A) enters the nucleus. The bound target protein is shuttled out of the nucleus along with the anchor protein.

Chapter 2
Materials and Methods

2.1. Strains and growth parameters

Table 2.1 lists all of the strains used in this study. For liquid cultures, Yeast extract peptone broth (1% Yeast extract and 2% peptone) was prepared and autoclaved. Sterile Dextrose (Glucose) solution was added aseptically to a final concentration of 2% Dextrose to prepare Yeast extract peptone dextrose (YEPD) broth. 5 ml of this media was inoculated with a single colony of yeast and grown overnight at 30°C in a shaking incubator at 200 RPM to prepare started cultures. A volume of this started culture was sub-inoculated into a greater volume of YEPD broth and was grown under the same conditions until the log phase was attained (Optical density between 0.3-0.8 on the spectrophotometer). YEPD agar (2% agar) was used as a solid medium.

2.2. Protein extraction

A method described by (Szymanski and Kerscher 2013) was used to isolate total protein from the yeast cells. A mid-log phase culture was grown. 10 OD units were harvested and centrifuged at 376g for 5 minutes. The supernatant was discarded, and the pellet was resuspended in 1 ml 20% TCA. It was then transferred to a new 1.5ml tube and centrifuged at 16,363 g for 15 s, and the supernatant was discarded. The pellet obtained could be stored at -20°C beyond this point. It was resuspended in 250 µl 20% TCA and ~500 mg of 500-600 µm glass beads (Sigma) were added. This mixture was mechanically agitated in a Maxiprep 3 times for the 30s each with 1 minute of cooling on ice between each blast. The lysate was then transferred to a new 1.5 ml tube with a sequencing tip to avoid transferring glass beads. The beads were washed with 500 µl 5% TCA and the aqueous portion was transferred to the same 1.5 ml tube. The lysate was incubated on ice for 3 minutes and centrifuged at 16,363 g for 1 minute. The

supernatant was discarded, and pellet fully resuspended in 300 μ l of 1X Laemmli [0.1 % β -mercaptoethanol, 10 % glycerol, 2 % SDS & 63 mM Tris-Cl (pH 6.8)].

This suspension was boiled at 95°C for 5 minutes followed by centrifugation at 16,363g for 1 minute. The supernatant was transferred to a new 1.5 ml tube.

2.3. Total protein quantitation

The extracted protein was quantified using Bradford's assay according to the manufacturer's instructions (Sigma). A portion of the lysate was diluted 5000x with ultrapure water. Standards of 2,4,6,8 and 10 μ g/ml were prepared with Bovine Serum Albumin (BSA). Bradford's reagent was added to the samples, standards and the blank. Absorbance was measured at a wavelength of 595 nm on a spectrophotometer. The protein concentration of the samples was interpolated using a standard curve generated using absorbance values of the BSA standards. The working stocks of the protein samples were adjusted to a concentration of 2 mg/ml with 1X Laemmli and stored at -20°C.

2.4. RNA extraction

The RNA extraction procedure was adapted from a protocol described in current protocols (Collart and Oliviero 1993). Cells were grown to log phase (OD ~0.3), and a 10 ml culture was harvested and pelleted by centrifugation for 2 minutes at 202 RCF. The pellet was resuspended in 1ml of sterile ultrapure water and transferred to a clean 1.5 ml Eppendorf tube. This suspension was then centrifuged at 8978 RCF for 3 minutes. The pellet was stored at -80°C. This was labelled as the time-zero sample. Rapamycin was added to the culture to a final 1 μ g/ml concentration. Cells were

similarly harvested, pelleted, and stored at 10 minutes, 20 minutes, 40 minutes, 60 minutes, 2 hours, 4 hours and 6 hours post the addition of rapamycin.

The pellet was resuspended in 400 μ l of TES solution (10 mM Tris-Cl pH 7.5, 10 mM EDTA, 0.5% SDS). A further 400 μ l buffer saturated acid-phenol was added and the suspension was vigorously vortexed for ~15 seconds. The suspension was then incubated at 65°C for one hour with occasional vortexing. The samples were cooled on ice for 5 minutes and centrifuged at 16,363 RCF for 5 minutes at 4°C. The aqueous phase (top layer) was transferred to a clean 1.5 ml Eppendorf tube and 400 μ l of buffer saturated acid-phenol was added. The tubes were vigorously vortexed for ~15 seconds, cooled on ice for 5 minutes and centrifuged at 16363 RCF for 5 minutes at 4°C. The aqueous phase (top layer) was transferred to a clean 1.5 ml Eppendorf tube and 400 μ l of Chloroform was added. The tubes were vigorously vortexed for ~15 seconds and centrifuged at 16363 RCF for 5 minutes at 4°C. The aqueous phase (top layer) was transferred to a clean 1.5 ml Eppendorf tube. 40 μ l of DEPC-treated 3M Sodium acetate (pH 5.3) and 1 ml of ice-cold absolute ethanol were added. The samples were incubated at -20°C for the RNA to precipitate. The suspension was centrifuged at 16,363 RCF for 10 minutes at 4°C. The supernatant was discarded, and the pellet was washed with 1 ml of ice-cold 70% ethanol. The suspension was centrifuged at 16,363 RCF for 5 minutes at 4°C. All the supernatant (ethanol) was removed with a micropipette followed by drying at 37°C until no traces of ethanol could be observed in the tubes. The precipitated RNA was resuspended in 50 μ l of nuclease-free water. A 10 μ l aliquot was collected to measure the concentration of the isolated RNA using a NanoDrop ND-100 spectrophotometer (Thermo Scientific) measured at an absorbance wavelength of 260 nm (A₂₆₀ nm). The remaining RNA was stored at -80°C.

2.5. RNA visualization under denaturing conditions on an agarose-formaldehyde gel

To inspect the extracted mRNA, a 1.5% (w/v) agarose gel was prepared by dissolving 1.8g agarose in 86.4 ml dH₂O by boiling. The solution was cooled to 60°C in a water bath. 12 ml of 10X MOPS running buffer [0.4 M MOPS (3-(N-morpholino)-propanesulfonic acid), pH 7.0, 0.5 M sodium acetate and 0.01 M EDTA) and 21.6 ml of 40% formaldehyde were added. The gel was poured and allowed to solidify before being transferred to a gel tank. 1X MOPS running buffer was added to completely immerse the gel.

A total of 10 µg RNA was loaded into each well of the gel. The volume of each RNA sample was adjusted up to 10µl with nuclease-free water. 25µl MMF (500µl formamide, 162µl formaldehyde (40%) and 100µl 10X MOPS), and 2µl EtBr were then added to each sample. The samples were mixed and incubated at 60°C for 15 min then left on ice. 5µl loading dye was added to each sample and loaded on the prepared gel. The gel was run at 70V for the first 15 minutes and at 100V for the remaining duration.

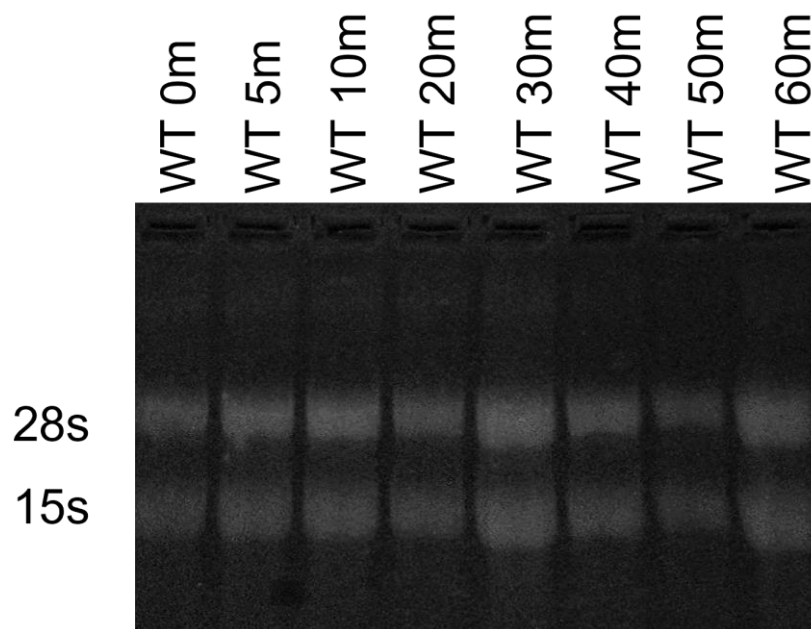


Figure 6. RNA visualization under denaturing conditions. A short time course from 0-60 minutes of WT mRNA to visualize the 28S and 15S RNA bands.

2.6. DNase treatment and cDNA generation

The RNA samples were first treated with RQ1 RNase-free DNase (Promega). 2 μ g RNA was incubated with 1 unit of DNase in 1X reaction buffer at 37°C for 1 hour. Then, 1 μ l of stop solution (20 mM EDTA) was added and the samples were incubated at 65°C for 10 minutes.

Reverse transcription (RT) was performed on the DNase-treated RNA samples to generate cDNA using a High-capacity RNA to cDNA kit (Applied Biosystems). 1 μ g of DNase-treated RNA was incubated with 1 unit of Reverse Transcriptase in 1X reaction buffer at 37°C for 1 hour. The reaction was stopped by incubating at 95°C for minutes and held at 4°C. Negative RT controls were carried out by replacing Enzyme Mix with DEPC-treated water

The generated cDNA samples were stored at -20°C.

2.7. Real-time qPCR

The template DNA for the qPCR was either diluted cDNA for transcription analysis or diluted IP/Input DNA for ChIP analysis. The cDNA and the IP DNA were diluted appropriately to fit within the standard curve. The qPCR protocol was adapted from current protocols (Bookout et al. 2006). For transcription analysis, a 20µl reaction contained 1X Applied Biosystems Power SYBR Green (Thermo), 150nM of each primer, 2µl template DNA and dH₂O to 20µl. qPCR was analysed by relative quantification using a standard curve on an Applied Biosystems Step One Plus real-time PCR system. The expression of the target gene was measured relative to *ACT1*, a reference gene selected based on previously published data (Pathan et al. 2017). Its expression was found to be stable in all the strains throughout the time course. qPCR was performed using a 20µl reaction containing 1X Applied Biosystems Power SYBR Green (Thermo), 150nM of each primer, 2µl template DNA and dH₂O to 20µl. qPCR on ChIP experiments was analysed using PCR-purified Ips and inputs.

For ChIP analysis, the input DNA was diluted 50X and the IP DNA was diluted 4X. qPCR was performed using a 20µl reaction containing 1X Applied Biosystems Power SYBR Green (Thermo), 150nM of each primer, 2µl template DNA and dH₂O to 20µl. qPCR on ChIP experiments was analysed using PCR-purified IPs and inputs. The expression was measured by comparing the IP levels, which reflect the protein occupancy at a given region, to the input levels, which reflect the total DNA in the sample. These IP/Input values were also normalised to a telomeric control region TEL VI.

| Name | Sequence | Description | Distance from ATG |
|----------------|--------------------------------|---|-------------------|
| TEL VI-R 121 F | CGTGTGTAGTGATCCGAACTCAGT | Control region | N/A |
| TEL VI-R 121 R | GACCCAGTCCTCATTCCATCAATAG | | |
| PMA1 ORF-F | GAAAAAGAATCTTTAGTCGTTAAGTTCGTT | Control region | +322 |
| PMA1 ORF-R | AATTGGACCGACGAAAAACATAA | | |
| ACT1 ORF-F | GAGGTTGCTGCTTTGGTTATTGA | Control region | +318 |
| ACT1 ORF-R | ACCGGCTTTACACATACCAGAAC | | |
| FLO1RT-F | TACCACCACAGACGGGTTCT | <i>FLO1</i> Transcription /ChIP (ORF) | +481 |
| FLO1RT-R | CAACAGTTGAACGCGGTTGC | | |
| SUC2RT486-F | AGCTGCCAACTCCACTCAAT | <i>SUC2</i> transcription/ ChIP (ORF) | +486 |
| SUC2RT486-R | ATTTGGCAGCCGTCATAATC | | |
| IPFLO3-F | GCTTCCAGTATGCTTTCACG | <i>FLO1</i> ChIP (promoter) | -585 |
| IPFLO3-R | GCCTACGTATTCTCCGTCAC | | |
| NUC2-F | CGCATTTTTTACTCTGAACAGG | <i>SUC2</i> ChIP (promoter) | -473 |
| NUC2-R | GGACGTGGGGTCGATTAAC | | |

Table 1 Oligonucleotides used in this study.

2.8. Sodium Dodecyl Sulphate - Polyacrylamide gel electrophoresis (SDS-PAGE)

10% and 12% (v/v) polyacrylamide resolving gels were prepared using the BioRad Mini-PROTEAN Cell system [10% (v/v) and 12% (v/v) acrylamide (Protogel, National Diagnostics), 0.38 M Tris-Cl (pH8.8), 0.001 % (w/v) SDS, 0.001 % (w/v) ammonium persulfate (APS) & 0.001% (v/v) N,N,N,N - Tetramethylethylenediamine (TEMED), based on the required resolution for the protein. The resolving gels were immediately overlaid with 1 ml of Isopropanol to prevent oxidation and allow for polymerization. The isopropanol was discarded once the gel was set. 6% (v/v) stacking gel [6 % (v/v) acrylamide, 78 mM Tris-Cl (pH 6.8), 0.001% (w/v) SDS, 0.001% (w/v) APS & 0.001% (v/v) TEMED] was poured. The gel plate was then sealed with a 10-toothed plastic comb inserted anaerobically at the top to allow for polymerization. 30 µg of

protein was boiled at 95°C for 5 minutes and loaded into the appropriate wells. The first and the last wells were loaded with a 10-170 kDa protein ladder. The gels were run for 120 minutes at 100V in running buffer [25 mM Tris, 190 mM glycine, 0.1 % (w/v) SDS].

2.9. Western Blotting

The protein was transferred from the SDS-PAGE gel to the polyvinylidene fluoride (PVDF)

membrane (Immobilon) in transfer buffer (25 mM Tris, 190 mM glycine & 20% (v/v) methanol) at 300 mA for 40 minutes at 4°C (Bio-rad, Mini trans-blot, 153BR). A transfer sandwich was constructed in the following order: 2X sponges, 1X filter paper, SDS-PAGE gel, PVDF membrane, and 1X filter paper. The sponges, filter papers and the SDS-PAGE gel were all soaked in transfer buffer. The PVDF membrane was soaked in Methanol for 20s and dH₂O for 2 minutes just before use. After transfer, the membrane was incubated in blocking buffer [5% (w/v) dried skimmed milk in Tris-buffered saline with 0.05% (v/v) Tween

20 (TBST, Sigma)] for 1 hour, rocking at room temperature. The membrane was then incubated with the primary antibody diluted to the appropriate concentration (Table) overnight at 4°C. After incubation, the membrane was washed with TBST 4 times for 5 minutes. Secondary HRP-conjugation antibodies were diluted to the appropriate concentration (Table 2) in blocking buffer and incubated with the membrane for 90 min at room temperature. After incubation, the membrane was washed for 10 min in TBST followed by 3 washes of 10 min in TBS (TBS, Sigma). The bound antigens were detected using enhanced chemiluminescent (ECL) Western Blotting Substrate (Pierce)

according to the manufacturer's instructions. The Imagequant las 4000 imager was used to develop the membrane.

| Protein | Concentration | Species | Source |
|----------------|----------------------|----------------|--------------------|
| β -actin | 1:3000 | Mouse | Abcam (ab8224) |
| FRB | 1:2000 | Rabbit | Enzo ALX-215-065-1 |
| Myc | 1:5000 | Mouse | Millipore (05-724) |

Table 2 Primary antibodies used in the western blots

2.10. Chromatin Immunoprecipitation (ChIP)

2.10.1. Cell growth and cross-linking

A starter culture was prepared by inoculating 5 ml YEPD with a single colony and incubated overnight at 30°C agitating at 200 RPM. The following day, 450 ml of YEPD was inoculated with the starter culture and was grown to an OD of ~0.3. 100 ml of culture was collected in a 250 ml conical flask and was processed as the time-zero sample. Formaldehyde (Sigma, 37%) was added to a final concentration of 1% and was left for 20 minutes with shaking for cross-linking. To quench this reaction, 50mM of glycine was added to the cultures and shaken for a further 5 minutes. Cross-linked cultures were transferred to a 50 ml centrifuge tube and centrifuged at 1000 rcf for 5 minutes at 4°C. The supernatant was discarded, and the cell pellet was resuspended in 25 ml ice-cold TBS. Cells were pelleted by centrifugation at 1000 rcf at 4°C and the supernatant was discarded. The TBS wash was repeated, and cell pellets were stored at -80°C.

Rapamycin was added to the culture to a final 1 µg/ml concentration. Cells were similarly harvested and cross-linked at 30 minutes, 60 minutes, 2h and 4h post addition of the Rapamycin. 10mM EDTA was added to flocculant cells to disperse the flocs.

2.10.2. Preparation of cell lysates

Cross-linked cell pellets from 2 x 50 ml cultures from each time-point were each resuspended in 400 µl FA lysis buffer (50mM HEPES, 140 mM NaCl, 1mM EDTA, 1% Triton X-100, 0.1% sodium deoxycholate) supplemented with a 1:100 dilution of protease inhibitor cocktail (PI) (Sigma P2714- 1BTL, resuspended according to manufacturer's instructions) and 2 mM 75 phenylmethylsulphonyl fluoride (PMSF) (Sigma). Then 500 µl of acid-washed or zirconia beads (BioSpec Products, Inc) were added to each tube. Cells were lysed by extensive vortexing using the Maxiprep for 4 X 30-second blasts with 1 minute on ice in between blasts. The lysate was transferred to a new 1.5 ml tube with a syringe needle tip and made up to 1 ml with FA lysis buffer.

The lysate was pulse centrifuged to settle the bubbles and any pellet formed was gently resuspended into the lysate.

The lysates were then sonicated in a Sanyo Soniprep 150 sonicator. Each sample was subjected to 12 pulses of 10 seconds each at an amplitude of 8 microns, with 1 minute on ice between each 10-second pulse. The lysates were then clarified by centrifugation at 16,363 rcf in a microcentrifuge for 30 minutes at 4°C. The supernatant was transferred to a new 1.5ml tube and aliquots equivalent to 5 or 10 OD volumes were made. The lysate was stored at -80°C.

2.10.3. DNA fragment size estimation

To check DNA fragment size after sonication, a proportion of sonicated lysate equivalent to 2 OD units of the original cell culture was protease-treated. Samples were protease-treated by incubating with protease (Sigma) and 1:1 sample: protease ratio with 1% CaCl₂ at 42°C for 2 hours. Crosslinks were reversed by incubation at 65°C overnight. Phenol-chloroform DNA extraction was performed on lysate. Half of each sample was run on a 1.5% agarose/TBE gel. The fragmented DNA was compared against a 100-1500bp DNA ladder to confirm that the DNA fragment length was within that range.

2.10.4. Immunoprecipitation (IP)

The cross-linked and sonicated lysates were defrosted on ice and made up to 500 µl with FA lysis buffer containing PI at a concentration of 1:10000 PI: FA Lysis buffer. The samples were mixed gently by inverting the tubes and 20µl was taken from each as the input. Inputs were protease-treated by adding 100 µl ChIP elution buffer (25 mM Tris-Cl [pH 7.5], 5 mM EDTA, 0.5 % SDS), 5 mM CaCl₂ and 2 mg/ml protease type XIV (Sigma) to each 20 µl input sample and bringing the mixture to 200 µl with 60 µl TE (pH 7.5). These samples were incubated at 42°C for 2 hours and crosslinks were reversed by incubating at 65°C for 6 hours. They were then purified using a Qiagen QiaQuick PCR purification kit as per the manufacturer's instructions.

The appropriate Antibody (Table 3) was added to the remaining 480 µl lysate and incubated with rotation at 4°C overnight. The following morning, a mixture of 20 µl of Protein A magnetic dynabeads (Invitrogen) and 20 µl of Protein G magnetic dynabeads (Invitrogen) per sample. The beads were washed by suspending the mix in 1 ml of FA lysis buffer + PI followed by rotation at 16 RPM at room temperature. The tubes were then

attached to a magnetic stand (DynaMag-2 Magnet) and the supernatant was pipetted away. This wash was repeated two more times. The antibody + lysate solution was then added to the washed beads and incubated with rotation for 2 hours at 4°C.

The antibody-bead complexes were washed in 1ml FA lysis buffer for 5 minutes, followed by two washes in 1 ml ChIP wash buffer 1 [50 mM HEPES (pH 7.5), 0.5 M NaCl, 1 mM EDTA, 1 % Triton X-100, 0.1 % Sodium deoxycholate], two washes in 1 ml ChIP wash buffer 2 [10 mM Tris-Cl (pH 8.0), 0.25 M LiCl, 1 mM EDTA, 0.5 % NP-40, 0.5 % Sodium deoxycholate] and a single wash in 1 ml TE (pH 7.5). Beads were bound to a magnet and supernatant was aspirated and discarded between washes.

The antibody-bead complexes were resuspended in 250 µl ChIP elution buffer (25 mM Tris-Cl [pH 7.5], 5 mM EDTA, 0.5 % SDS) and vortexed vigorously. This was followed by incubation at 65°C at room temperature, rotation for 10 minutes at room temperature and centrifugation at 16,363 rcf for 1 minute. The supernatant was transferred to a new 1.5 ml tube for protease treatment.

To protease-treat IP samples, 3mg/ml protease and 5mM CaCl₂ were added, and the solution was incubated at 42°C for 2 hours. Cross-links were reversed by incubation at 65°C for 6 hours. Ips 38 were purified using a QiaQuick PCR purification kit (Qiagen) according to the manufacturer's instructions.

| Antibody | Pre-bind? | Number of washes | The volume of antibody per IP | Protein A or G | Source |
|-----------------|------------------|-------------------------|--------------------------------------|-----------------------|--------------------|
| Pol II | No | 2 | 4.5 μ l | A/G mix | Covance (MMS-126R) |
| Tup1 | No | 2 | 1.5 μ l | A | J. Reese |
| Myc | No | 2 | 2.5 μ l | G | Millipore (05-724) |

Table 3 Antibodies used in ChIP

Chapter 3

Preliminary data

Previous work in the lab had studied *FLO1* and *SUC2* gene transcription in *tup1*, *cyc8* and *tup1 cyc8* gene deletion mutants. The data suggested that *FLO1* and *SUC2* were subject to distinct regulation by the Tup1-Cyc8 complex (Fig. 7 – Unpublished data from B. Lee, Fleming Lab).

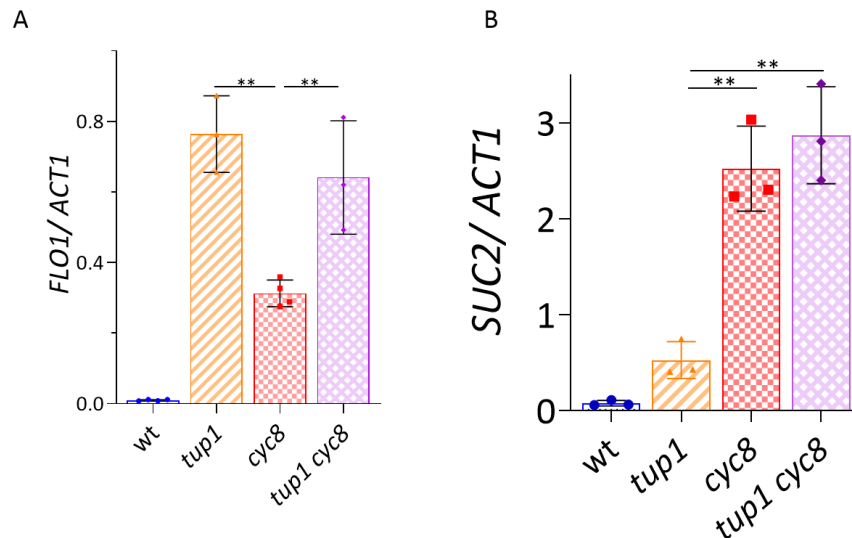


Figure 7. The *FLO1* and *SUC2* transcription profiles in *tup1* and *cyc8* gene deletion mutants. Values are normalised to *ACT1* mRNA and error bars reflect standard deviation (* represents a p-value of $p < 0.05$, ** represents a p-value of $p < 0.005$ determined by a Student's t-test).

As can be seen in fig. 7, *FLO1* transcription is absent in WT cells due to Tup1-Cyc8 repression. However, in a *tup1* deletion mutant *FLO1* is de-repressed to a greater extent than that seen in the *cyc8* deletion mutant. Interestingly, when *tup1* is additionally deleted in the *cyc8* mutant, the level of de-repression is the same as that seen in the *tup1* single mutant. Together, this suggests a dominant role for *TUP1* in the repression of *FLO1* transcription and that *TUP1* can exert a repressive effect in the absence of Cyc8p.

When *SUC2* transcription was examined in the same glucose-grown deletion mutant strains the data showed that the opposite result was seen. At *SUC2*, de-repression is the

greatest in the *cyc8* gene deletion mutant compared to de-repression in the *tup1* gene deletion mutant. This suggests a greater role for Cyc8p in the repression of *SUC2*. The fact that *SUC2* de-repression in the double gene deletion mutant is similar to that seen in the *cyc8* single mutant suggests that *CYC8* can exert a repressive effect upon *SUC2* in the absence of Tup1p.

My project aimed to examine *FLO1* and *SUC2* transcription and associated events in Cyc8p and Tup1p conditional mutants to get greater insight into the role of Tup1p and Cyc8p in the repression of *FLO1* and *SUC2*. I wanted to use the anchor away mutants to test the hypothesis that Tup1p can persist at *FLO1* in the absence of Cyc8p where it might directly exert Cyc8p-independent repression. Similarly, I wanted to test the hypothesis that Cyc8p can persist at *SUC2* in the absence of Tup1p where it might promote Tup1p-independent repression of *SUC2* transcription. I was hypothesizing that the use of conditional mutants for this analysis of the Tup1p and Cyc8p function would be superior to the analysis of the Tup1-Cyc8 function using gene deletion mutants due to the decreased likelihood of secondary effects occurring in the conditional mutants.

Chapter 4

Characterization of the Anchor-away strains

4.1. Introduction

Rapamycin is toxic to conventional wild-type yeast. Haruki et al. used strains rendered resistant to Rapamycin by mutating *TOR1* (*tor1-1*) and deleting the *FPR1* gene. The wild-type strain used in this study was similarly made Rapamycin resistant and was referred to as 'HHY221' or 'WT'.

The Tup1 Anchor-away (Tup1AA) is a WT strain with an FRB tag attached to the Tup1p protein (constructed previously by B. Lee from the Fleming lab). Similarly, the Cyc8p Anchor-away (Cyc8AA) is a WT strain with an FRB tag attached to the Cyc8p protein (constructed previously by M. Church from the Fleming lab). The addition of Rapamycin triggers the depletion of the target protein from the nucleus. My first experiment was to confirm the strains were correct.

4.2. Confirmation of the FRB tag

A Western blot was performed on the protein extracts of WT and the Tup1-AA and Cyc8-AA strains using the anti-FRB primary antibody (Table 2). The aim was to confirm the presence of the FRB tag on the Tup1p and the Cyc8p proteins in the respective anchor-away strains. The FRB tag has a MW of ~ 11 KDa. Thus, Tup1-FRB was expected to weigh ~ 90 KDa and Cyc8-FRB was expected to be ~120 KDa. β -actin was used as a loading control. Fig. 8 depicts the result of the Western blot.

The FRB tag was detected in the Tup1AA and the Cyc8AA strains and gave a band of the expected sizes. No band was detected in the WT. Therefore, the Tup1-AA and Cyc8-AA strains were confirmed as being correctly constructed.

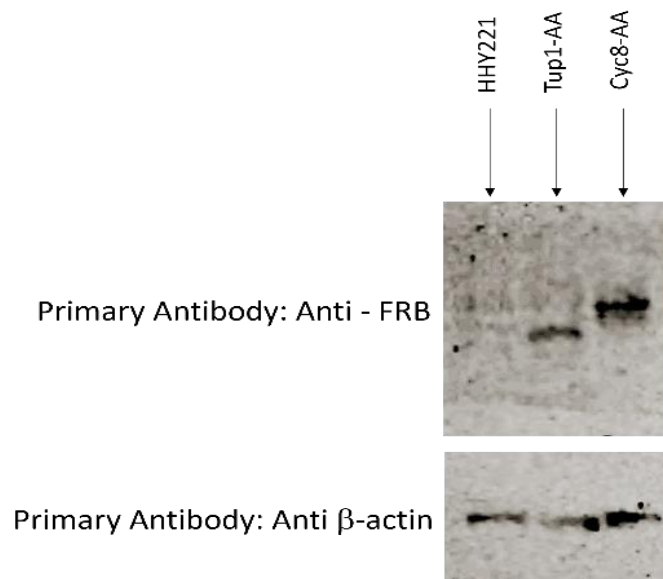


Figure 8. **Western Blot to detect the FRB tag on the AA strains** Protein lysates (30ug protein) from colonies from WT (HHY221), Tup1AA and Cyc8AA strains were loaded. β -actin was used as a loading control.

4.3. Visualizing the flocculant phenotype in Tup1-AA and Cyc8-AA cells following rapamycin addition

The *FLO1* gene is repressed in most laboratory WT yeast strains by the Tup1-Cyc8 complex (Fleming and Pennings 2001). Conversely, strains deleted for *CYC8* and *TUP1* display a strong flocculation phenotype due to loss of repression by Tup1-Cyc8. This offers an easy assay by which to determine Tup1p and Cyc8p function. It was therefore expected that the addition of Rapamycin to the anchor away strains at the log phase would trigger the flocculent phenotype in the cells if the anchor away technique was functional and if Cyc8p and Tup1p were removed from the nucleus. The flocculation phenotype in WT, Tup1-AA and Cyc8-AA cells was therefore tracked for 6 hours post the addition of Rapamycin (Fig. 9) by looking for evidence of cell sedimentation due to flocculation in tissue culture plates.

In the Tup1-AA cells, flocculation was first observed 2 hours after the addition of rapamycin to the medium. Based on observation by the naked eye, the flocculation peaked at the 4h mark and remained uniform until the end of the time course. Like the Tup1AA cells, flocculation was first observed 2 hours after the addition of Rapamycin to the medium in the Cyc8AA cells. Based on naked-eye observation, the flocculation in the Cyc8-AA cells peaked at the 5h mark and remained uniform until the end of the time course. There was no flocculation visible in the WT cells following rapamycin addition.

EDTA chelates Ca^{2+} ions and acts as an inhibitor to flocculation (Stratford 1992). The experiment was thus repeated in the presence of 10mM EDTA, which works as a control to

confirm if the cell sedimentation observed was due to flocculation or not (Fig. 10). Upon the addition of EDTA to the samples taken after 6h incubation with rapamycin, there were no flocs visible in the Tup1-AA and Cyc8-AA, and all samples looked identical to the WT. This suggests that the sedimentation phenotype observed in the Anchor-away strains was indeed due to flocculation.

Together, this suggests that the anchor-away technique was working and that Tup1p and Cyc8p were depleted from the nucleus following rapamycin addition.

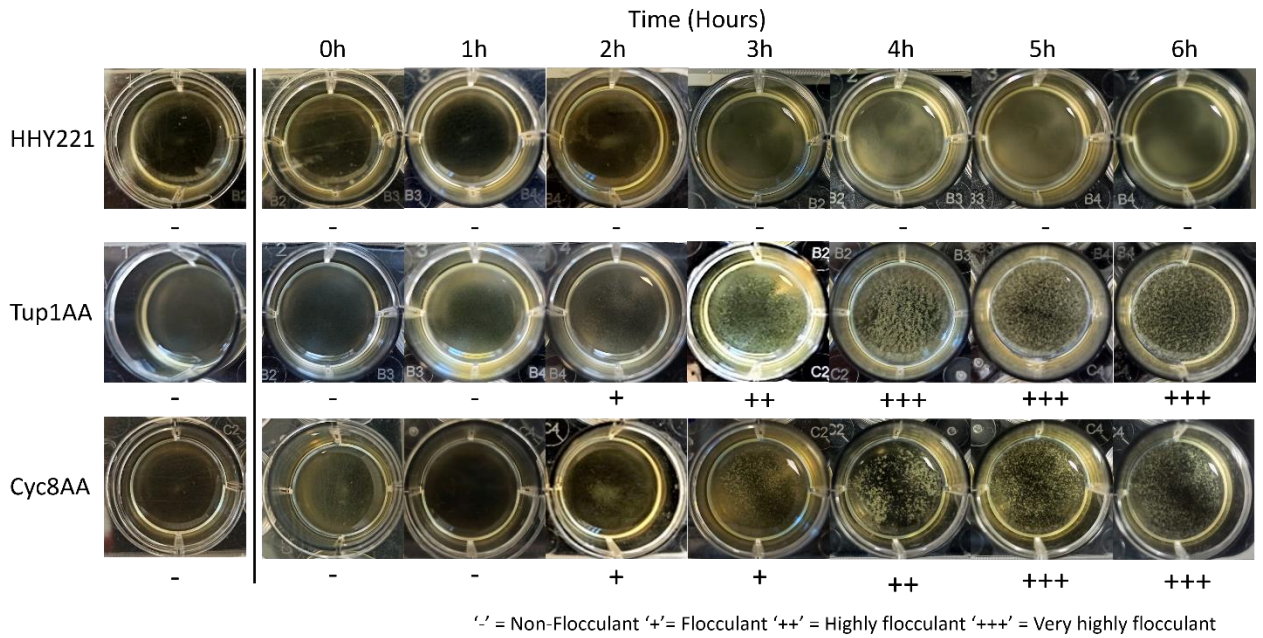


Figure 9. Observing flocculation over time. 1 ml of culture was aseptically transferred to a deep well plate before and after the addition of Rapamycin at 1-hour intervals until 6 hours.

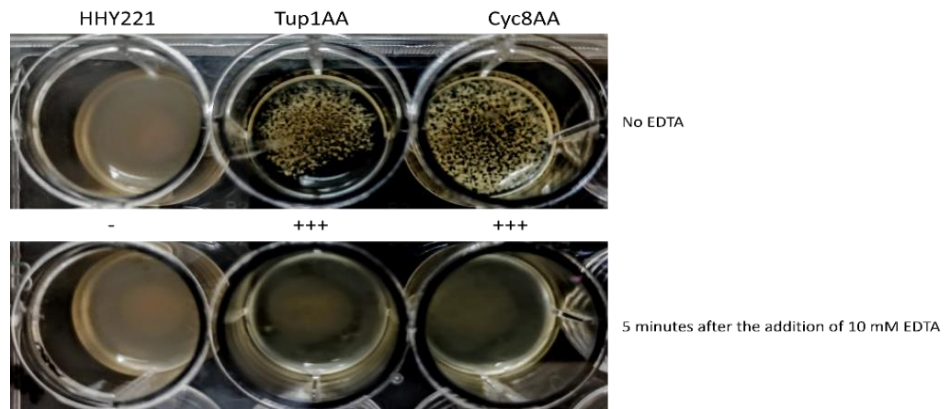


Figure 10. Flocculation control. Cells collected at 6h post-rapamycin addition, with (above) and without (below) the addition of EDTA.

Chapter 5

Investigating the role of the Tup1-Cyc8 complex in gene transcription

5.1. Examining *FLO1* transcription in Tup1-AA and Cyc8-AA strains

The *FLO1* gene is the dominant gene of the five-member *FLO* gene family and is independently capable of regulating flocculation in wild-type yeast (Smukalla et al. 2008). The *FLO1* gene should not be transcribed in WT strains due to repression by the Tup1-Cyc8 complex (Fleming and Pennings 2001). However, in Tup1-AA and Cyc8-AA strains following rapamycin addition, *FLO1* transcription should be de-repressed due to the loss of Tup1p and Cyc8p from the nucleus. I therefore next examined *FLO1* transcription in Cyc8-AA and Tup1-AA strains over time after rapamycin addition. cDNA was prepared from cells collected before and several time points after the addition of rapamycin to the log phase cultures and was used as template DNA for RT-qPCR analysis (Fig. 11).

The data showed that *FLO1* gets significantly de-repressed two hours after the addition of rapamycin in the Tup1-AA strain and is de-repressed after four hours post rapamycin addition in the Cyc8-AA strain. While not significant compared to WT, there is a reproducible increase in *FLO1* expression in Cyc8AA two hours post-rapamycin addition (Fig. 11). This supports the previous phenotypic observation where flocculation was visible in the anchor-away strains two hours after the addition of rapamycin (see fig. 9). Consistent with the lack of flocculation in WT cells exposed to rapamycin, *FLO1* gene transcription was not detected in the WT strain at any time point after rapamycin addition.

It is also worth noting that the *FLO1* gene transcription in the Cyc8-AA strain is over two-fold higher than that seen in the Tup1-AA strain at each of the 2, 4 and 6h time points. Thus, *FLO1* transcription is de-repressed by 2 hours after rapamycin addition in both the Tup1-AA and Cyc8-AA strains. However, the de-repression of *FLO1* is consistently higher in the Cyc8-AA strain than the de-repression observed in the Tup1-AA strain at all time

points tested. This suggests a greater role for Cyc8p in the repression of *FLO1* transcription.

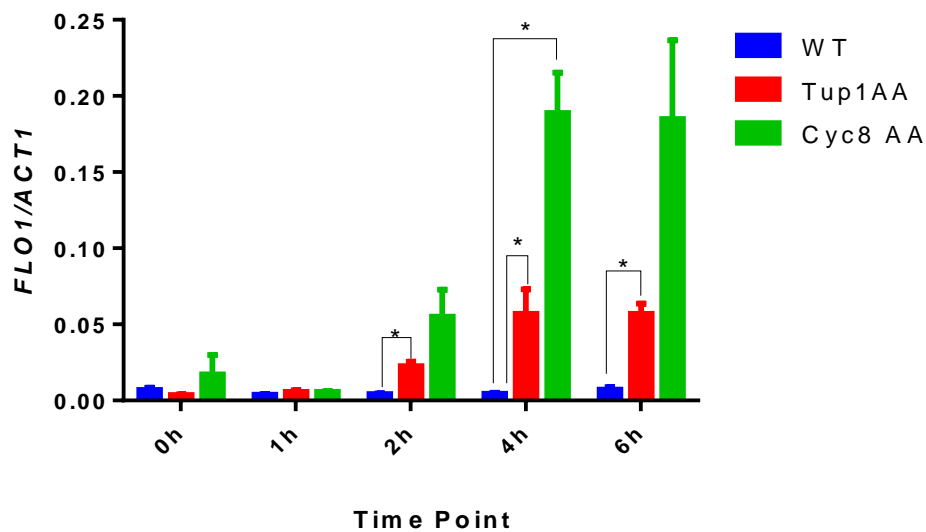


Figure 11. *FLO1* expression measured using RT-qPCR in the anchor-away time-course. Values are normalised to *ACT1* mRNA and error bars reflect standard error of mean (SEM) (* represents a p-value of $p < 0.05$, ** represents a p-value of $p < 0.005$ determined by a Student's t-test).

5.2. Examining *SUC2* transcription in Tup1-AA and Cyc8-AA strains

The invertase-encoding *SUC2* gene is also known to be under the transcriptional control of the Tup1-Cyc8 complex (Fleming and Pennings 2007). Invertase is required for the hydrolysis of sucrose into glucose and galactose and is subject to Tup1-Cyc8 dependent glucose repression. This predicts that *SUC2* transcription should be off in WT and should be on in cells depleted for Tup1p and Cyc8p. I, therefore, analysed *SUC2* transcription over time in the WT, Tup1-AA and Cyc8-AA strains following rapamycin addition. The prediction would be that *SUC2* would be de-repressed over time after rapamycin addition.

The transcription data showed that *SUC2* gets significantly de-repressed in the Cyc8AA and Tup1-AA strains by 1-hour post-Rapamycin addition (Fig. 12). Similar to what was seen for the *FLO1* gene (Fig. 11), de-repression of *SUC2* was greatest in the Cyc8-AA strain at each time point tested compared to the level of de-repression seen in the Tup1-AA strain. No signal for *SUC2* transcription was detected in WT at any time point. Together, this is consistent with Cyc8p again having the greatest repressive role upon *SUC2* transcription.

5.3. Examining *SUC2* transcription in Tup1-AA and Cyc8-AA strains over a finer time-course

In the previous examination of *SUC2* transcription in the Cyc8-AA and Tup1-AA strains, the data suggested that the rate of *SUC2* de-repression was faster than that seen for *FLO1* following rapamycin addition. Furthermore, the data suggest that *SUC2* transcription levels in the Tup1-AA strain might have already peaked by 1-hour post rapamycin addition. I, therefore, chose to repeat the analysis of *SUC2* transcription, but over a shorter time

course, to get a finer time course analysis of *SUC2* de-repression following Tup1p and Cyc8p depletion from the nucleus (Fig. 13).

The data revealed significant de-repression of the *SUC2* gene was observed at 40 minutes post-rapamycin addition in the Cyc8-AA and Tup1-AA strains. While depression was observable in the Tup1-AA strain at as early as 20 minutes in the time-course, it was not statistically significant. There was also no further significant increase in *SUC2* levels in the Tup1-AA and Cyc8-AA strains in the later time points compared to 40 minutes after rapamycin addition. No signal for *SUC2* transcription was detected in WT at any time point. Thus, maximum *SUC2* de-repression seems to occur by 40 min post rapamycin addition. Similar to what was seen before for the longer *SUC2* de-repression time course, and for the de-repression of *FLO1* in the anchor-away strains, the level of *SUC2* de-repression in the Cyc8-AA strain was always greater than that seen in the Tup1-AA strain. This is consistent with Cyc8p contributing the most to *SUC2* and *FLO1* gene repression.

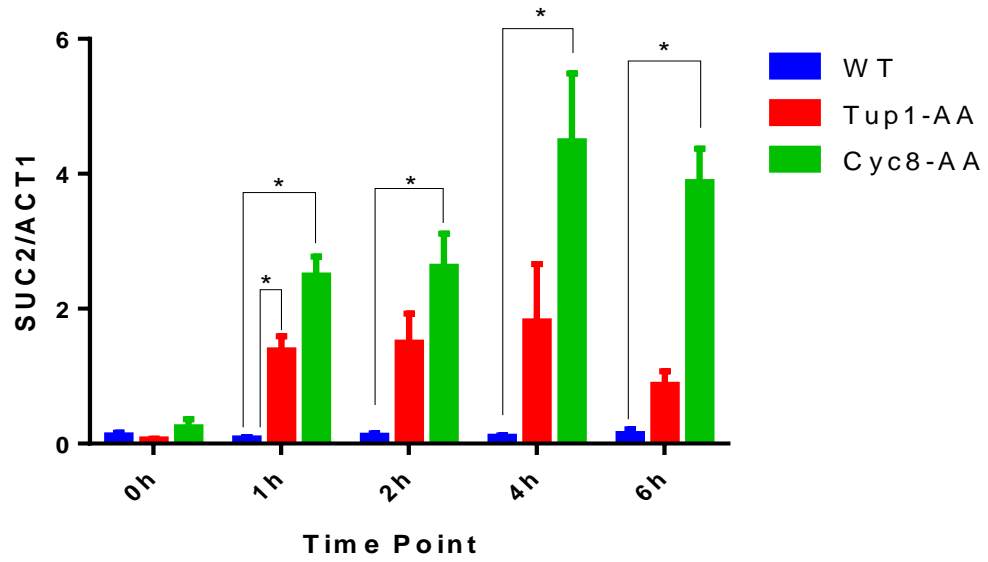


Figure 12. *SUC2* expression measured using RT-qPCR in the anchor-away time-course. Values are normalised to *ACT1* mRNA and error bars reflect SEM (* represents a p-value of $p < 0.05$, ** represents a p-value of $p < 0.005$ determined by a Student's t-test).

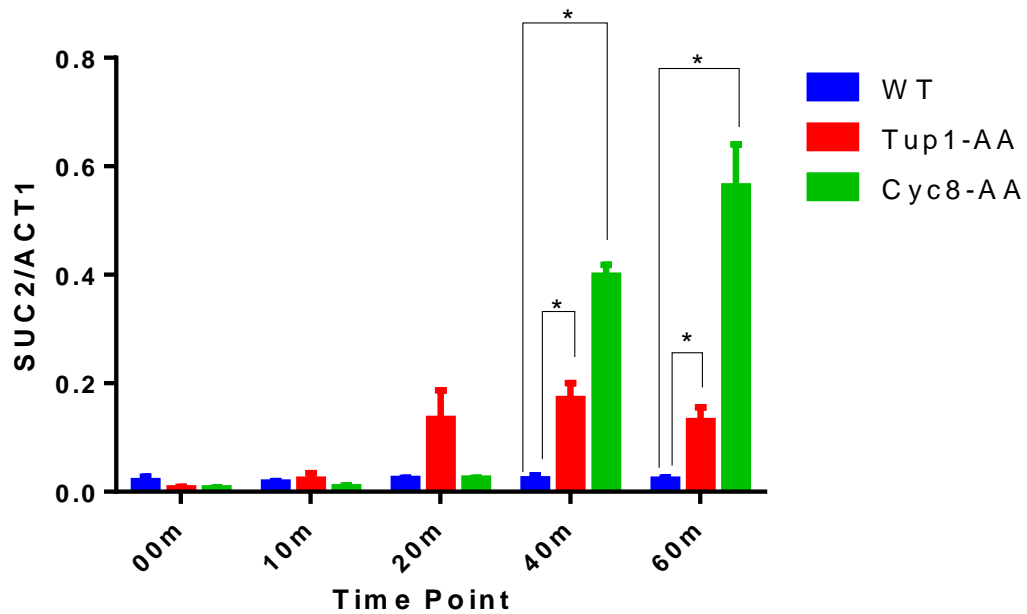


Figure 13. *SUC2* expression measured using RT-qPCR in a finer anchor-away time-course. Values are normalised to *ACT1* mRNA and error bars reflect SEM (* represents a p-value of $p < 0.05$, ** represents a p-value of $p < 0.005$ determined by a Student's t-test).

5.4. Examining *SEDI* transcription in Tup1-AA and Cyc8-AA strains

A recent study in the Fleming lab showed that the cell wall glycoprotein Sed1p encoding *SEDI* gene was under the transcriptional control of the Tup1-Cyc8 complex (Byrne 2020).

The transcription data (Fig. 14) showed that *SEDI* was abundantly and consistently expressed in the WT and both anchor away strains throughout the time course following rapamycin addition. However, despite the apparent increase in *SEDI* transcription in the Tup1-AA strain, there was no significant de-repression observed in either of the anchor-away strains throughout the time course compared to WT. Thus, this gene was not analysed further in this study.

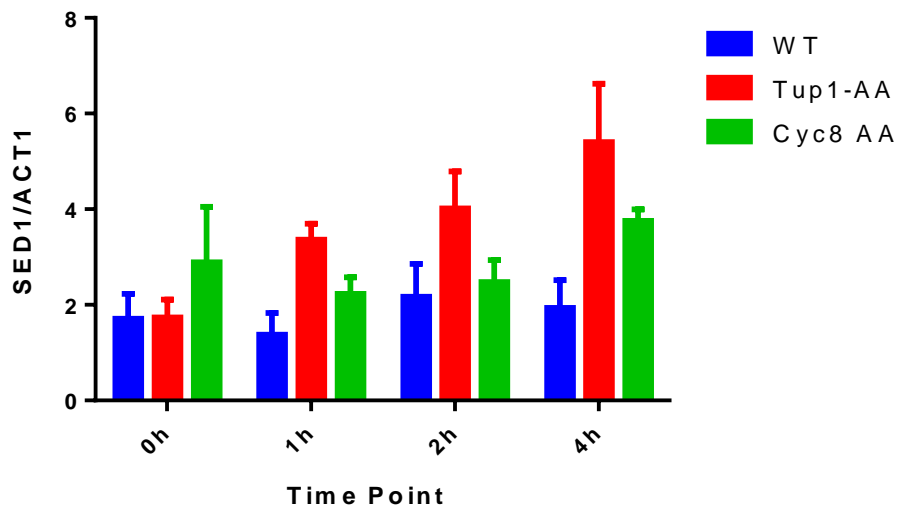


Figure 14. *SED1* expression measured using RT-qPCR in the anchor-away time-course. Values are normalised to *ACT1* mRNA and error bars reflect SEM

5.5. *PMA1* transcription is not de-repressed in Cyc8-AA and Tup1-AA strains following rapamycin addition

The *PMA1* gene encodes for the protein Pma1p, a vital plasma membrane protein. *PMA1* is known to be highly and constitutively transcribed in exponentially growing yeast strains. *PMA1* gene transcription is also not subject to regulation by the Tup1-Cyc8 complex. I, therefore, monitored the transcription of this gene as a control to determine whether the de-repression seen at the *FLO1* and *SUC2* genes was specific and was not due to a general increase in all gene transcription in cells treated with rapamycin.

The results (Fig. 15) showed that *PMA1* transcription in the Tup1-AA and Cyc8-AA strains were equally high at each of the time points tested after rapamycin addition and that these levels were similar to the levels in WT. This suggests that the de-repression of *FLO1* and

SUC2 seen in the Tup1-AA and Cyc8-AA were gene-specific and were not a consequence of a general increase in transcription in cells exposed to rapamycin.

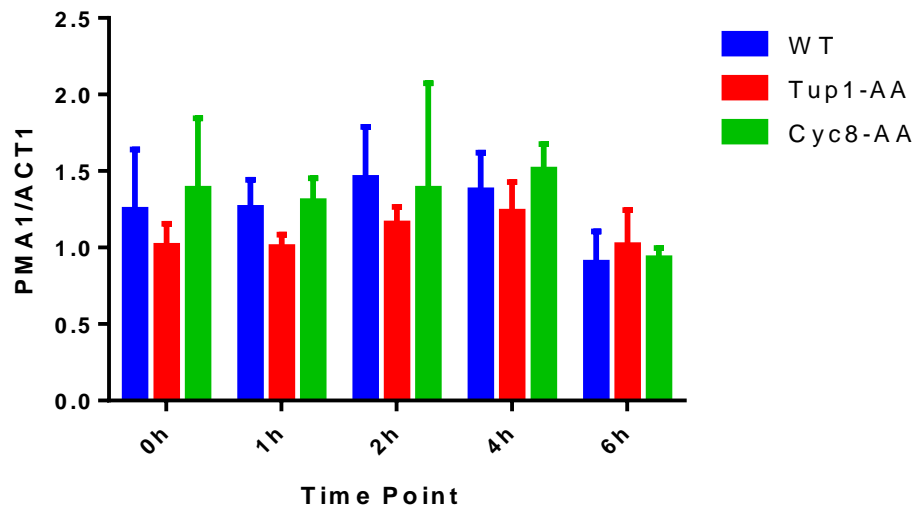


Figure 15. *PMA1* expression measured using RT-qPCR in the anchor-away time-course. Values are normalised to *ACT1* mRNA and error bars reflect SEM

5.6. Discussion

This analysis aimed at obtaining insights into the functioning of the Tup1-Cyc8 complex at genes known to be subject to Tup1-Cyc8 dependent repression.

Previous studies in gene deletion mutants showed that *FLO1* was most de-repressed in a *tup1* mutant whilst *SUC2* was most de-repressed in a *cyc8* gene deletion mutant. This suggested that *FLO1* was subject to most repression by Tup1p and that *SUC2* repression was dominated by Cyc8p. This suggested that the complex may not be functioning uniformly across all the genes under its influence. These data also raised the possibility of distinct repression of *FLO1* transcription by Tup1p and distinct repression of *SUC2* by Cyc8p. The variety of DNA-binding proteins which recruit the complex to target genes in their upstream control regions suggests that perhaps the different subunits of the complex can be independently recruited, or independently stimulated to repress target genes, to bring about this differential repressive effect. The aim of my first experiments in the anchor-away strains was to examine what the impact upon *FLO1* and *SUC2* transcription would be and to see if the AA strains behaved in a similar way to the gene deletion strains.

However, the de-repression of *FLO1* in the anchor away strains did not recapitulate the de-repression seen in the deletion mutant study. Indeed, most de-repression was observed in the Cyc8-AA strain. Conversely, *SUC2* was most de-repressed in the Cyc8-AA strain which was a similar result to that seen in *cyc8* deletion mutant strains. Thus, the anchor-away mutants are not de-repressing genes in a similar manner to that observed in gene deletion mutants. Indeed, for the two genes tested here, depletion of Cyc8p led to the highest de- of both *FLO1* and *SUC2*.

The role of the Tup1-Cyc8 complex in the transcription of the *FLO1* gene is well-characterized. Thus, *FLO1* serves as an ideal experimental control for examining Tup1-Cyc8 mediated repression. A previous study in the Fleming lab on the Cyc8AA strain revealed a similar trend in *FLO1* de-repression to what I observed (Church 2015), whereby *FLO1* transcription was first detected at 2 hours post-Rapamycin addition.

While *FLO1* was significantly de-repressed in the Tup1AA strain, de-repression was significantly higher in the Cyc8AA strain. These data open up two possibilities. Firstly, Tup1p is strongly bound to Cyc8p and the depleting of the DNA binding site of Cyc8p also depletes Tup1p to relieve repression and allow maximal de-repression. The second possibility is that in the Tup1-AA strain following Tup1p depletion, Cyc8p can persist at *FLO1* and can exert some independent repression upon *FLO1*. This is however, not universal; as the complex is known to employ different mechanisms at different targets. For instance, it has previously been reported that Cyc8p deletion had a negligible on Tup1 mediated transcription of *STE6* in terms of RNAPII occupancy (Wong and Struhl 2011).

The Sucrose utilization enzyme invertase coding *SUC2* gene was also studied previously in a Cyc8AA strain (Church 2015). *SUC2* was noted to be significantly de-repressed at 40 minutes post-Rapamycin addition in both AA strains.

At *SUC2*, similar to what was seen in gene deletion mutants, and similar to what was seen at *FLO1* in my anchor away strains, de-repression was the greatest in the Cyc8-AA strain. This is in keeping with the model of Tup1-Cyc8 repression which would predict that in the absence of Cyc8p, Tup1p should not be present, and we would therefore expect to see maximal de-repression. This is indeed what I see at *FLO1* and *SUC2* in the anchor-away

strains. This raises the question as to what is happening in the *tup1* and *cyc8* gene deletion mutant strains to give an opposite result, at least for *FLO1* de-repression. I would suggest that the anchor-away strains offer a truer reflection of the impact of the loss of Tup1p and Cyc8p, whereas it is secondary effects in the gene deletion mutants that cause the discrepancy in the de-repression seen at *FLO1*. This would predict that in *CYC8AA* strains Tup1p would not be present at either *FLO1* or *SUC2* after rapamycin addition. Similarly, my data would predict that Cyc8p persists at target genes in the Tup1-AA strains after rapamycin addition and that this Cyc8p can still contribute a Tup1p- independent repression activity.

Thus, in the next chapter, I aimed to directly test whether Tup1p is lost from target genes in a Cyc8-AA strain and whether Cyc8p persists at target genes in the Tup1-AA strain post rapamycin addition.

Chapter 6

Investigating the RNA Pol II, Tup1p and Cyc8p occupancy in the Tup1AA strain

6.1. Introduction

The previous chapter covered the effect of the Tup1-Cyc8 complex on gene transcription. To further attempt to understand the mechanism of action of Tup1-Cyc8, I performed a time-course analysis of RNAP II, Tup1p and Cyc8p at their respective binding sites of the target genes in the Tup1AA strain using the ChIP assay. The aim was to compare the data from the Tup1-AA time course to the data from a time-course ChIP assay that had already been performed on the Cyc8AA strain in a previous study in the Fleming lab (Church 2015). I wanted to test the hypothesis that Cyc8p persists at target genes in the absence of Tup1p.

Chromatin Immunoprecipitation (ChIP) was the assay of choice as it permits the study of protein-DNA interactions in-vivo within the context of the cells (Das et al. 2004). The ChIP assay used in this study involves formaldehyde-based DNA-protein cross-linking, subsequently quenched with glycine. This was followed by mechanical cell lysis facilitated by Zirconia beads. The lysate was then subjected to sonication to shear the DNA to 100-500 bp fragments. The fragmented DNA-protein complexes were then allowed to bind with the appropriate primary antibody and isolated from the lysate by precipitation with Protein A/G coated magnetic beads. The cross-links were then reversed by heat treatment and proteases were used to digest the proteins prior to a final DNA purification step. A qPCR reaction on the obtained immunoprecipitated (IP) DNA represents the occupancy of the protein it was immunoprecipitated with. All these steps are depicted in fig. 16.

The ChIP protocol is challenging, lengthy, contains several sources of variation and can be affected by artefacts occurring in the lysate. The ChIP signal is greatly influenced by the duration of formaldehyde crosslinking. A longer crosslinking step is reported to strengthen

the ChIP signal but may also result in crosslinking the protein-protein interactions, increased artefact levels and increased background levels. Another step which can significantly influence the downstream applications of ChIP is sonication. Despite the usage of protease inhibitors, sonication can still cause the degradation of proteins. Large proteins are more susceptible to degradation than smaller ones (Pchelintsev et al. 2016). ChIP assays have historically been characterized to be prone to high variability and low reproducibility. Thus, using ChIP to compare levels of different proteins at the same binding site rather than merely the detection has its pitfalls (Jonge et al. 2019).

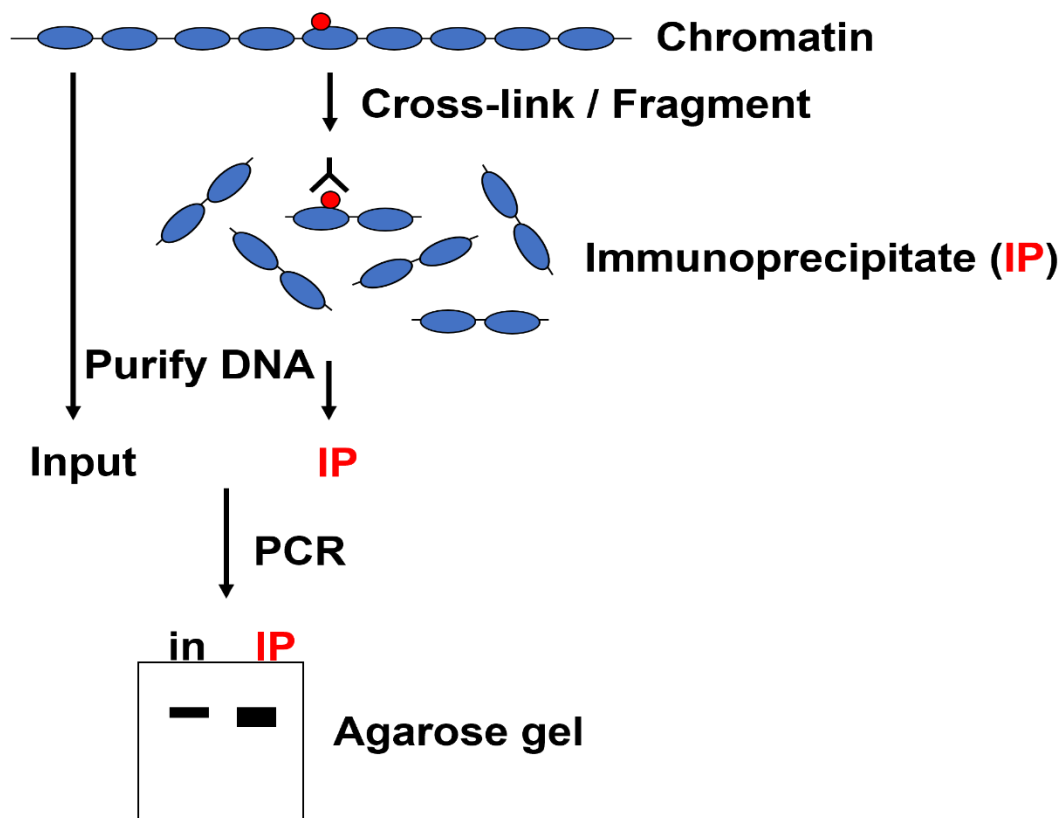


Figure 16. The ChIP assay The Chromatin and proteins are cross-linked with formaldehyde and the chromatin-protein complex is sheared by sonication. The now sheared DNA-protein complexes are immunoprecipitated with the desired antibody and the protein is digested. The target sequence (IP) is then detected by a qPCR and normalised to the input (in) qPCR signal using the same primers.

6.2. Confirming the Cyc8-myc strain

ChIP requires high-quality ChIP-grade antibodies for specificity. While there were suitable antibodies available for the detection of RNAP II and Tup1p, no ChIP- grade antibody was available for Cyc8p. Hence, a Tup1-AA strain was constructed in which the Cyc8 protein was tagged with an 11 KDa 9-myc tag. A ChIP grade antibody was then used against 9-myc to immunoprecipitate Cyc8-myc in the TUP1-AA strain before and after rapamycin addition.

Before starting the ChIP experiments, I confirmed that the Cyc8-myc construct was present and functional in the Tup1-AA strain. The figure represents western blot results from *S. cerevisiae* colonies obtained from a Cyc8-myc tagging attempt in the Tup1-AA strain background (labelled as TA 1 to TA6). The results showed that a band of the expected size (118 KDa) was present in the TA 5 and TA6 colonies only (Fig. 17). The lane labelled PC was the positive control which was a Cyc8-myc in a WT strain. As the signal in the 'TA6' colony yielded the strongest band, this strain was chosen for all the ChIP experiments.

I also confirmed that the function of Cyc8p following tagging was not impeded by the tag. If the tag on Cyc8p in the TA6 strain had inhibited Cyc8p function, we would predict that repression of the *FLO1* gene would fail, leading to a visible flocculation phenotype in TA6 cells grown without rapamycin. I, therefore, grew TA6 in YPD and assayed the cell culture for any visible flocculation phenotype. As demonstrated in figure 18, the tagged strain was non-flocculant, just like the WT. A *cyc8* deletion strain was used as a control to show flocculation.

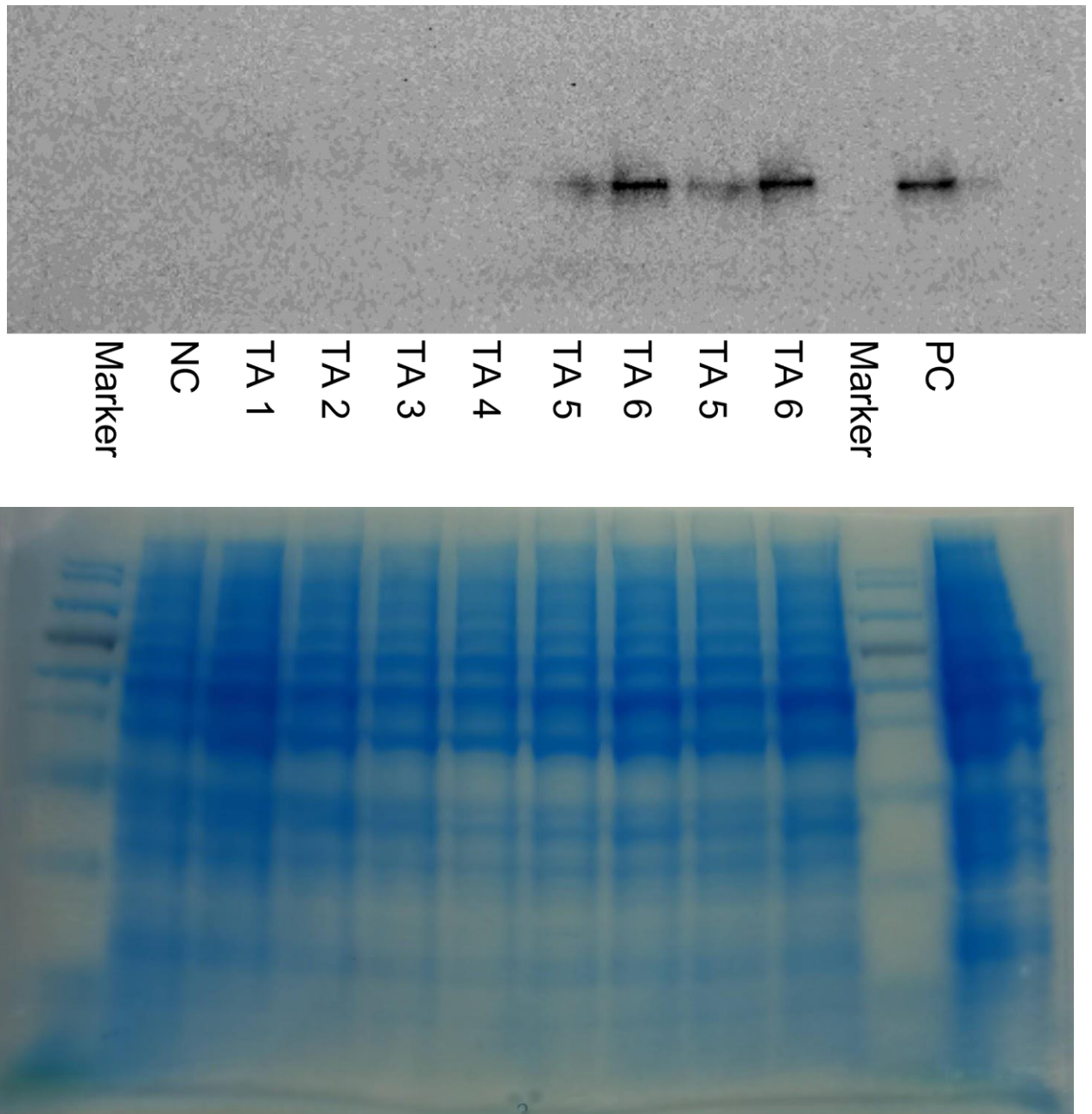


Figure 17. Western blot to confirm the myc tagging in the Cyc8-myc strain. Protein lysates (30 μ g protein) from colonies from TA 5 and 6 were loaded in duplicate for samples TA5 and TA6 since a previous western blotting attempt yielded a faint band for these lysates. NC is the negative control (WT lysate, no tag) and PC is the positive control which was Cyc8-myc in a WT strain. The size markers used (Markers) were visible on the membrane following transfer and were used to estimate the size of the positive band detected. The markers are not visible in the image shown above which is of the final resultant chemiluminescent signal. The image below is a Coomassie blue-stained gel with the same lysates used for the western blot loaded in the same order to act as a loading control.

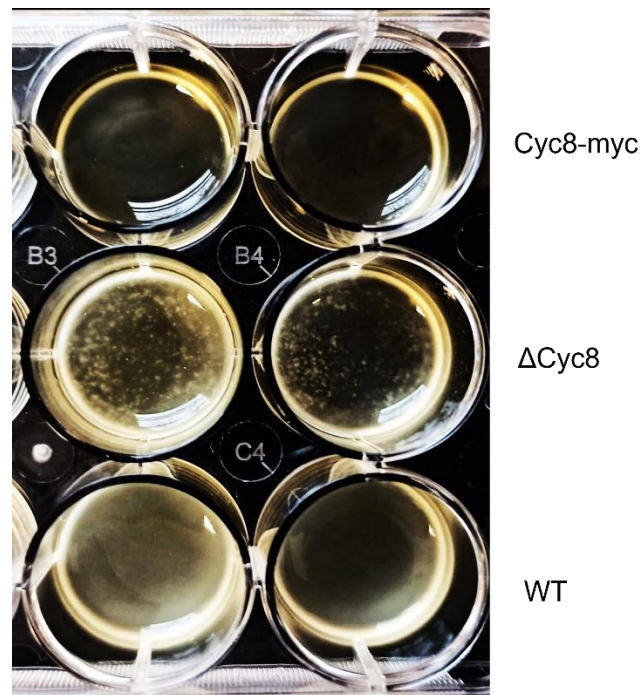


Figure 18. Confirmation of Cyc8p function in the Cyc8-myc Each row contains samples loaded in duplicate.

6.3. Optimizing the ChIP protocol

Prior to any IPs being performed all samples were analysed to confirm chromatin fragmentation by sonication had yielded a fragment length enriched around 500 bp (Fig. 19). Any lysates that did not reach this fragment length criterion were deemed unacceptable for further analysis and the experiment was repeated. All ChIP experiments were performed at least twice to yield at least two biological replicates per experiment.

The ChIP protocol was first attempted on WT samples with the aim to measure RNAP II occupancy at the ORFs of *PMA1* and *FLO1*. *PMA1* works as a target positive control and *FLO1* as a target negative control since its expression should be repressed by Tup1-Cyc8

in WT. Tel VI is a telomeric control region that also acts as an internal negative control for RNAPII occupancy. RNAPII occupancy (IP/in) at *PMAI* was observed to be almost 12-fold higher than at *FLOI* (Fig. 20, left-hand data). The plot on the right (Fig. 20) shows the normalization method whereby the IP/Input values for the target genes were divided by the IP/input values of Tel VI to give a ‘relative occupancy’ ChIP signal. All subsequent ChIP results were displayed as relative occupancy, whereby the target gene IP/in signal was normalized to the internal Tel VI negative control IP/input signal.

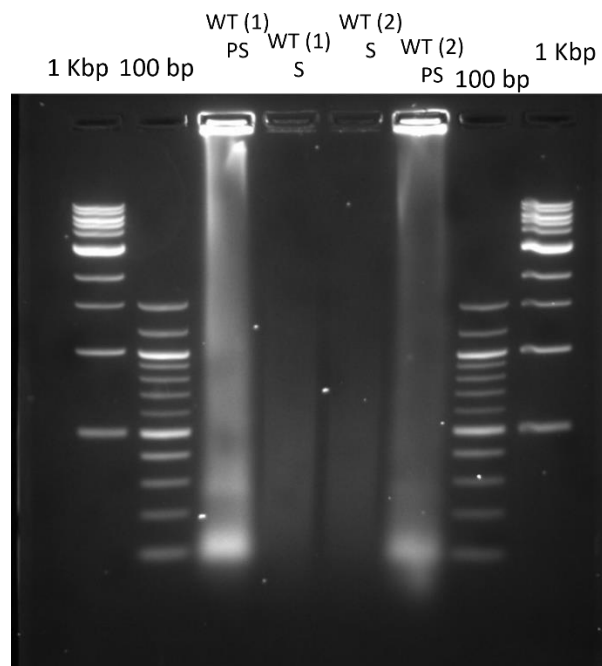


Figure 19. Sonication for chromatin fragmentation. Lanes 1 and 2 contain DNA ladders of 1 Kbp and 100 bp respectively. Lane 3 contains a PS (pre-sonication) sample of WT replicate 1, lane 4 contains an S (sonicated) sample of WE replicate 1. Lanes 5 and 6 contain S and PS samples of WT replicate 2 respectively. Lanes 7 and 8 contain DNA ladders of 100 bp and 1 Kbp respectively (Left to right).

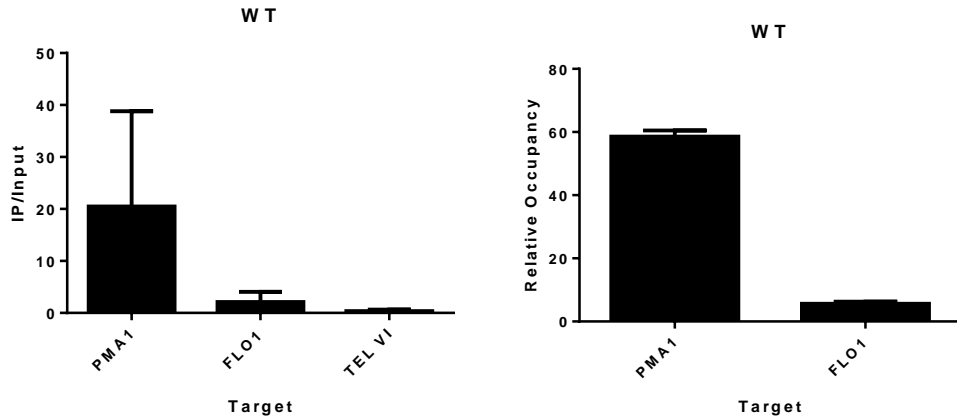


Figure 20. Target controls and the normalization method for ChIP assays. Ratio of IP/input amplification values following RNA Pol II ChIP in wt at target open reading frame regions (*PMA1* and *FLO1*) and the telomeric internal negative control (*TEL-VI*) region as measured by qPCR (left-hand data) (Error bars reflect SEM). *PMA1* and *FLO1* open reading frame IP/in amplification values following normalization to *TEL VI* IP/in values to show RNA Pol II ‘relative occupancy’ at the *FLO1* and *PMA1* open reading frames (right-hand data).

6.4. RNA Pol II occupancy at Tup1-Cyc8 repressed genes following Tup1p and Cyc8p depletion.

RNAP II levels were investigated at the open reading frames (ORFs) of Tup1-Cyc8 target genes as it has been shown that high Pol II occupancy at ORFs is known to correlate well with active transcription (Viktorovskaya and Schneider 2015).

I, therefore, performed a time course analysis to measure Pol II levels at genes known to be subject to Tup1-Cyc8 repression following rapamycin addition to Tup1-AA cells. Specifically, I took samples at 0 minutes, 30 minutes, 60 minutes, 2 hours and 4 hours post

addition of Rapamycin to the culture and performed the ChIP analysis and measured RNAP II occupancy at the *SUC2* and *FLO1* genes

6.4.1. RNA Pol II occupancy at the *FLO1* open reading frame

I first looked at Pol II occupancy at the *FLO1* gene coding region in the Tup1-AA samples before and after rapamycin addition (Fig. 21). The prediction would be that Pol II levels should increase across the *FLO1* gene over time following rapamycin addition. As can be seen at the *FLO1* ORF in the Tup1AA strain, the RNAP II occupancy level reproducibly peaked at 4h post-Rapamycin addition. This correlated well with the results from the sedimentation assay (Fig. 9) and the RT-qPCR analysis of *FLO1* (see Fig 11) in the Tup1-AA strains post rapamycin addition. It was interesting to note that RNAP II levels at time-zero were above zero, despite the transcription measured by RT-qPCR being near-zero at that point (see Fig. 11). A similar observation was noted in a previous study on the Cyc8AA strain, where RNAP II levels were greater than zero at time zero in a time-course experiment (Church 2015).

6.4.2. RNA Pol II occupancy at the *SUC2* open reading frame

I next analysed the same samples to measure Pol II occupancy at the *SUC2* gene ORF (Fig. 22). Interestingly, RNAP II occupancy at the *SUC2* ORF increased at a faster rate across the *SUC2* ORF compared to that seen at *FLO1* and also reached higher levels than that seen at *FLO1* following Tup1-AA. Indeed, the relative occupancy of RNAP II rises almost 40-fold between time-zero and 30 minutes. This result again aligned well with the *SUC2* transcription data measured in the RT-qPCR analysis (figs 12 & 13), where significant derepression was also observed at 40 minutes post Rapamycin-addition.

Together, the RNA pol II ChIP data at *SUC2* and *FLO1* confirmed that my ChIP technique was working and confirmed that Pol II is recruited to both *FLO1* and *SUC2* ORFs following Tup1p depletion from these genes' promoters via the anchor away technique in a profile consistent with that reported for these genes de-repression following the loss of Tup1-Cyc8 repression. The data suggests that following the loss of Tup1p from the *FLO1* and *SUC2* promoters, de-repression occurs faster and to a greater level at the *SUC2* gene.

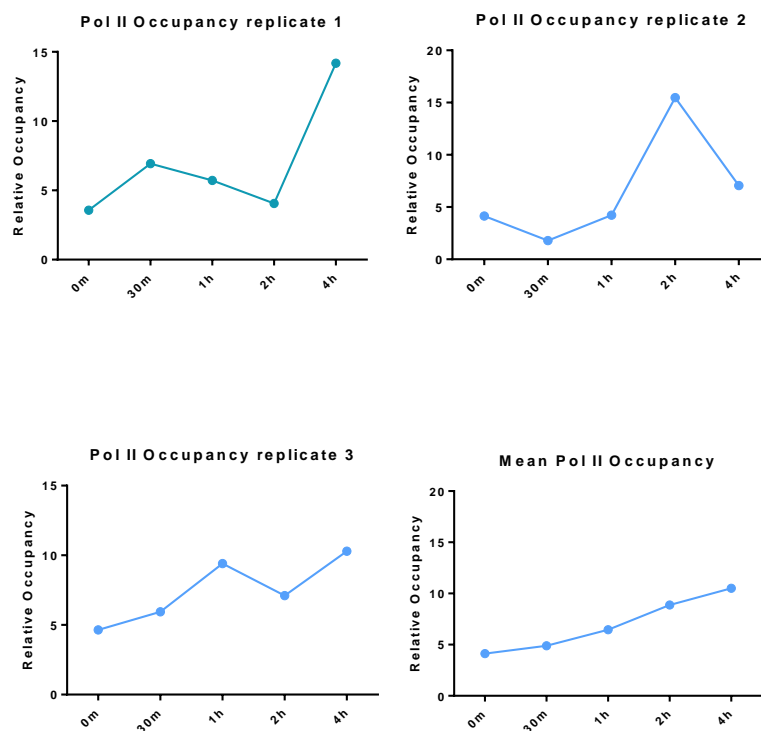


Figure 21. ChIP analysis of RNA Pol II occupancy at the *FLO1* open reading frame. All *FLO1* occupancy levels (at the *FLO1* ORF) are normalised to a telomeric control region (Tel V1). The plots shown are from each of the biological triplicate experiments (replicates 1 - 3), and the mean value of the triplicate experiments.

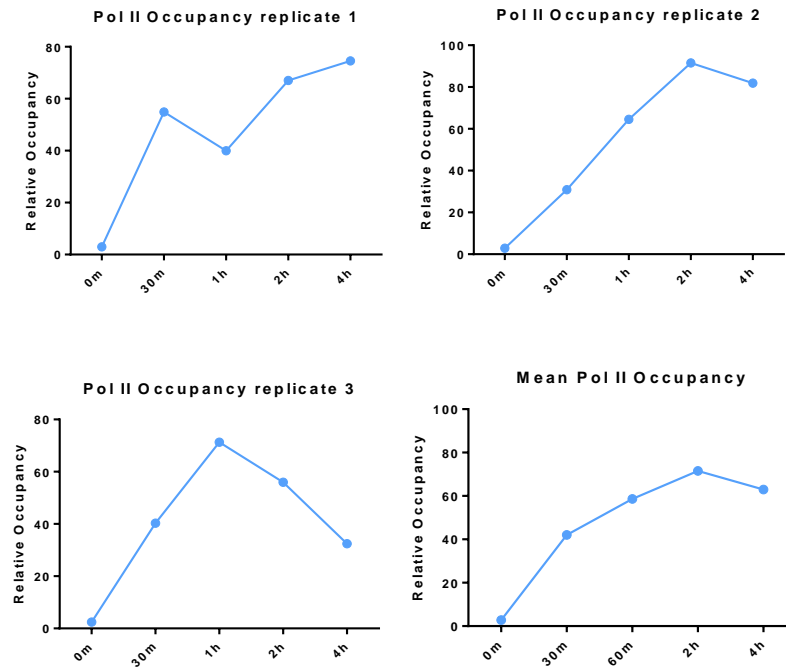


Figure 22. ChIP analysis of RNA Pol II occupancy at the *SUC2* open reading frame
 All *SUC2* ORF occupancy levels are normalised to a telomeric control region (Tel V1). The plots shown are from each of the biological triplicate experiments (replicates 1 - 3), and the mean value of the triplicate experiments.

6.5. Tup1p occupancy at the *FLO1* promoter in the Tup1-AA strain

At *FLO1*, The Tup1 protein is known to bind within the promoter region at about -585 bp upstream of the ATG start site; at the IPFLO3 site, to exert gene repression (Church et al. 2017). A largely predictable trend was observed with Tup1p occupancy in the Tup1AA time-course ChIP assay. Indeed, peak Tup1p occupancy in the *FLO1* promoter was detected at time-zero followed by a steady decline until 2 hours into the anchor-away time course after which, the level was the lowest. This observation is a direct reflection of the success of the anchor-away procedure and the Tup1 ChIP assay for the *FLO1* gene. Indeed,

it suggests that Tup1p is present at the repressed *FLO1* promoter and that Tup1p is lost from the promoter over time following the rapamycin induced depletion of Tup1p from *FLO1* via the AA technique.

6.6. Tup1p occupancy at *SUC2* in the Tup1-AA strain

Tup1-Cyc8 is known to occupy the *SUC2* promoter region indirectly via the Mig1p DNA-binding protein. The promoter region, which spans 600 bp upstream of the coding region, was characterized to contain four nucleosomes. Mig1p is known to be located at about – 442 bp upstream of the *SUC2* coding region and harbours the Tup-Cyc8 in the region corresponding to the second nucleosome (referred to as NUC2) (Boukaba et al. 2004). I, therefore, monitored Tup1p occupancy at this site in the *SUC2* promoter over time following Tup1-AA.

Unlike the results seen for Tup1p occupancy at *FLO1* in the Tup1-AA strain, the results at *SUC2* were intriguing. Contrary to predictions, Tup1p occupancy levels prior to rapamycin addition at the repressed *SUC2* gene were below the detection threshold. However, following 30 minutes post rapamycin addition, Tup1p could be detected above the background level. Tup1p occupancy at the *SUC2* promoter then declined again from this level over 1 and 2 hours post rapamycin time points and remained below the detection threshold at the 4 h time point.

These data suggest that Tup1p is undetectable at *SUC2* when the gene is repressed. However, upon Tup1 depletion, a peak of detection can be seen after 30 minutes post rapamycin addition, which then disappears over time to non-detectable levels.

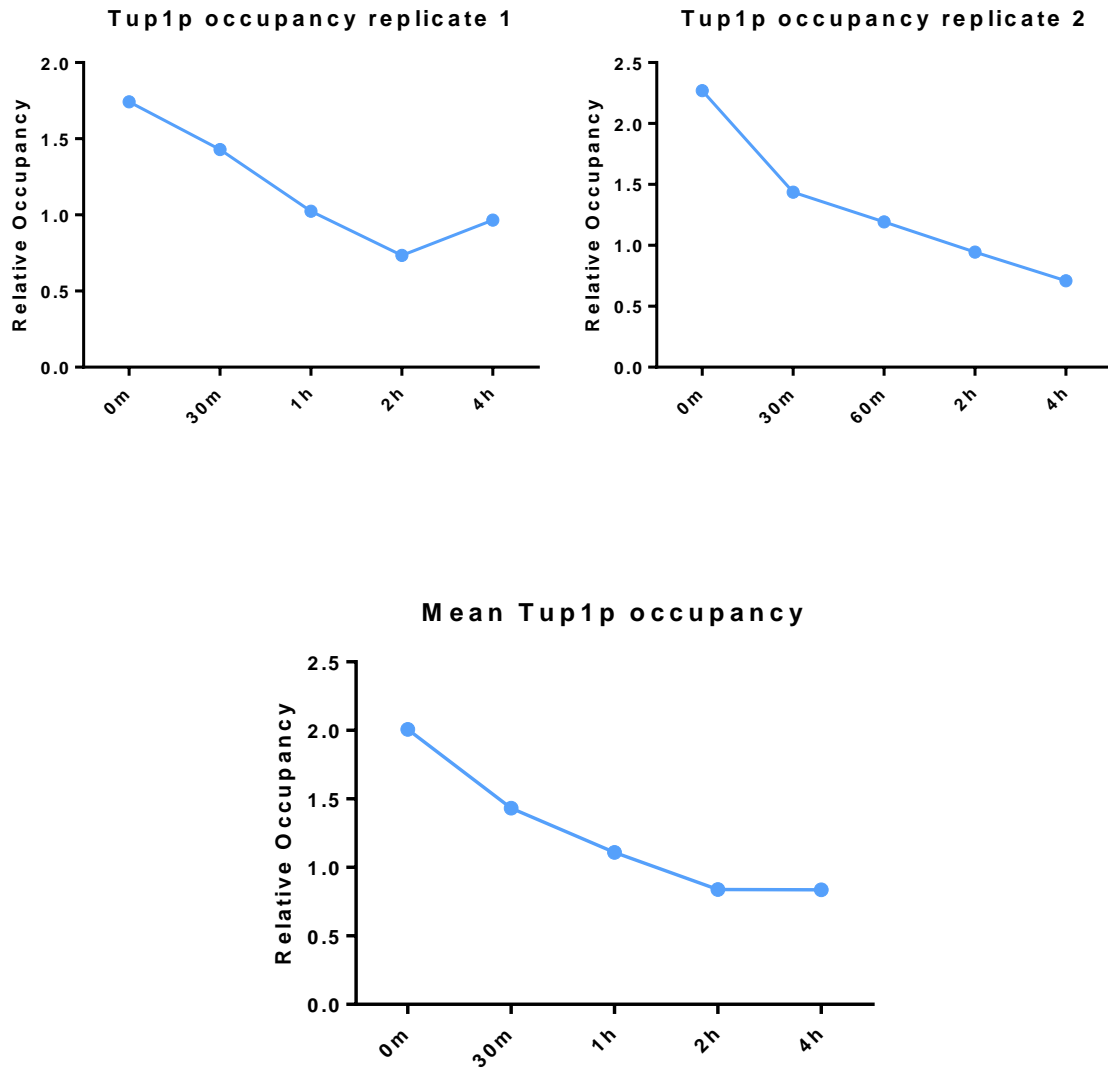


Figure 23. ChIP analysis of Tup1p occupancy at the *FLO1* promoter. All occupancy levels at the *FLO1* promoter are normalised to a telomeric control region (TEL V1). The plots shown are from each of the biological replicate experiments (replicates 1 - 2), and the mean value of the duplicate experiments.

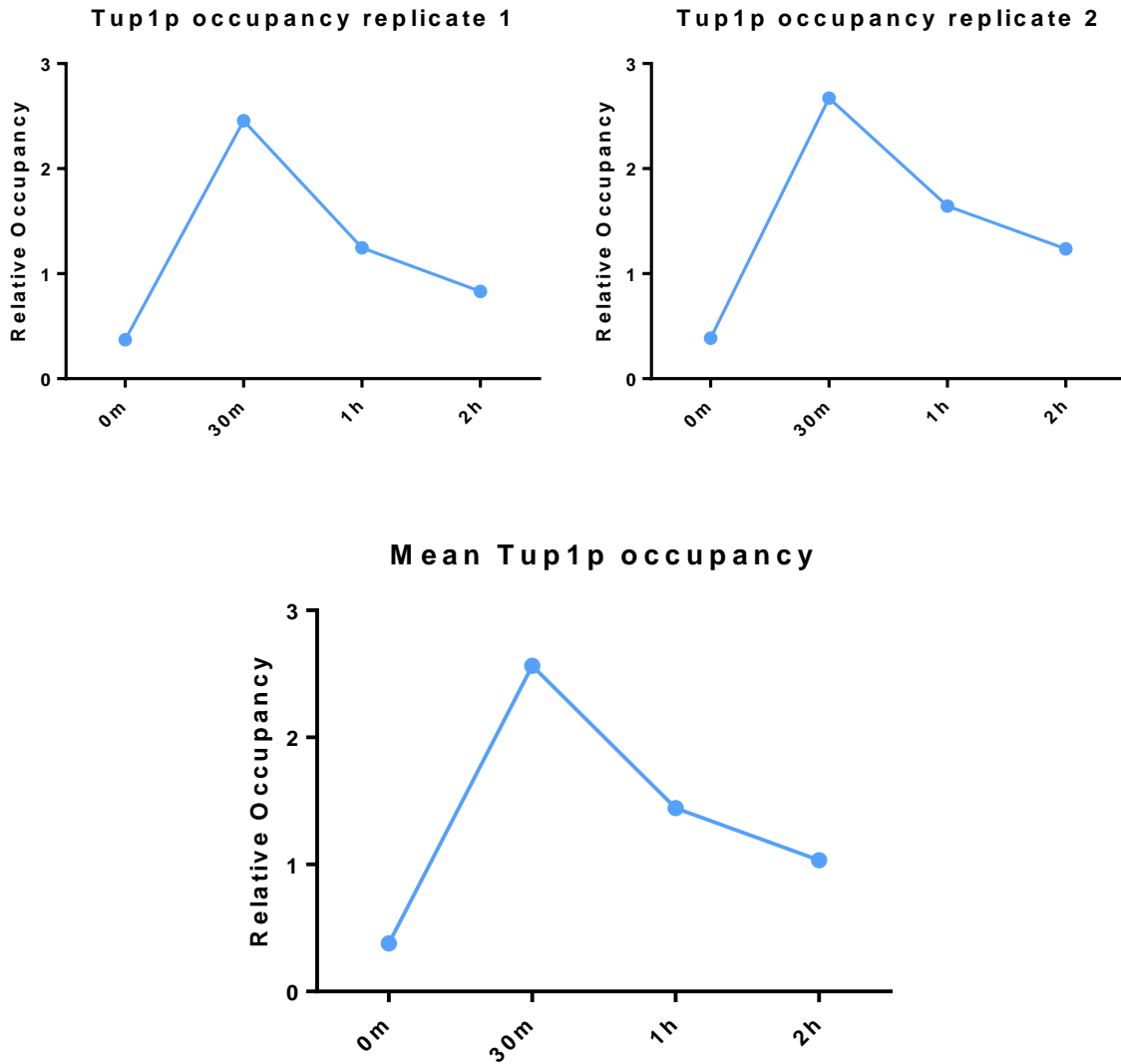


Figure 24 **ChIP analysis of Tup1p occupancy at the *SUC2* promoter** All occupancy levels at the *SUC2* promoter are normalised to a telomeric control region (TEL V1). The plots shown are from each of the biological replicate experiments (replicates 1 - 2), and the mean value of the duplicate experiments.

6.7. Cyc8-Myc occupancy at *FLO1* promoter in the Tup1-AA strain

The next objective was to study the effect of Tup1p depletion on Cyc8p occupancy. The regions of the promoters targeted for detecting Cyc8-myc were the same as for the Tup1p occupancy experiment. At the *FLO1* promoter, there was a small but reproducible Cyc8-myc signal detected above background at the repressed *FLO1* promoter before rapamycin addition. This is consistent with Tup1-Cyc8 occupying the *FLO1* promoter to promote gene repression. However, the signal was weaker than expected.

Following rapamycin addition and Tup1p depletion, and contrary to expectation, the signal detected for Cyc8p occupancy at the *FLO1* promoter reproducibly increased over time. Together, this showed that there was a weak signal for Cyc8p detected at the repressed *FLO1* promoter which then increased over time following Tup1p depletion from the *FLO1* promoter whilst *FLO1* transcription was de-repressed.

6.8. Cyc8-Myc occupancy at the *SUC2* promoter in the Tup1-AA strain

I next monitored Cyc8p occupancy at the *SUC2* promoter before and after Tup1p depletion via anchor away. The results showed that at *SUC2* before rapamycin addition, when the gene is repressed, Cyc8p occupancy could not be detected above background. This is again inconsistent with the expected result that would predict Tup1-Cyc8 should be present to mediate *SUC2* gene repression under these conditions. However, similar to what was observed for Cyc8p occupancy at the *FLO1* promoter, Cyc8p occupancy levels increased over time at the *SUC2* promoter following rapamycin addition. This suggests that at the repressed *SUC2* gene, Cyc8p occupancy could not be detected. However, following rapamycin induced Tup1p depletion, increasing amounts of Cyc8p levels could be detected above background as the gene became de-repressed.

6.9. Summary of Tup1p and Cyc8p ChIP data in the Tup1-AA strain

Together the data suggested that Tup1p and Cyc8p could be detected at the repressed *FLO1* gene promoter (prior to rapamycin addition). Upon rapamycin addition, Tup1p was lost from the *FLO1* promoter concomitant with *FLO1* gene de-repression. However, Cyc8p levels, as measured by ChIP, increased over time at the *FLO1* promoter following Tup1p depletion. Thus, Cyc8p persists, and possibly increases in levels at the *FLO1* gene during de-repression in the absence of Tup1p.

At *SUC2* on the other hand, neither Tup1p nor Cyc8p were detectable at the promoter when the gene was repressed (prior to rapamycin addition). This is contrary to the model for Tup1-Cyc8 repression of *SUC2* which would predict that Tup1p and Cyc8p should be present at the repressed *SUC2* gene promoter. Even more surprisingly, Tup1p occupancy was transiently detected at the *SUC2* promoter at the 30 min post rapamycin addition time point, during gene de-repression. However, this Tup1p occupancy signal was then lost again at the later post rapamycin time points during *SUC2* gene de-repression. Similar to what was seen at *FLO1*, Cyc8p ChIP levels at *SUC2* increased over time following Tup1p depletion.

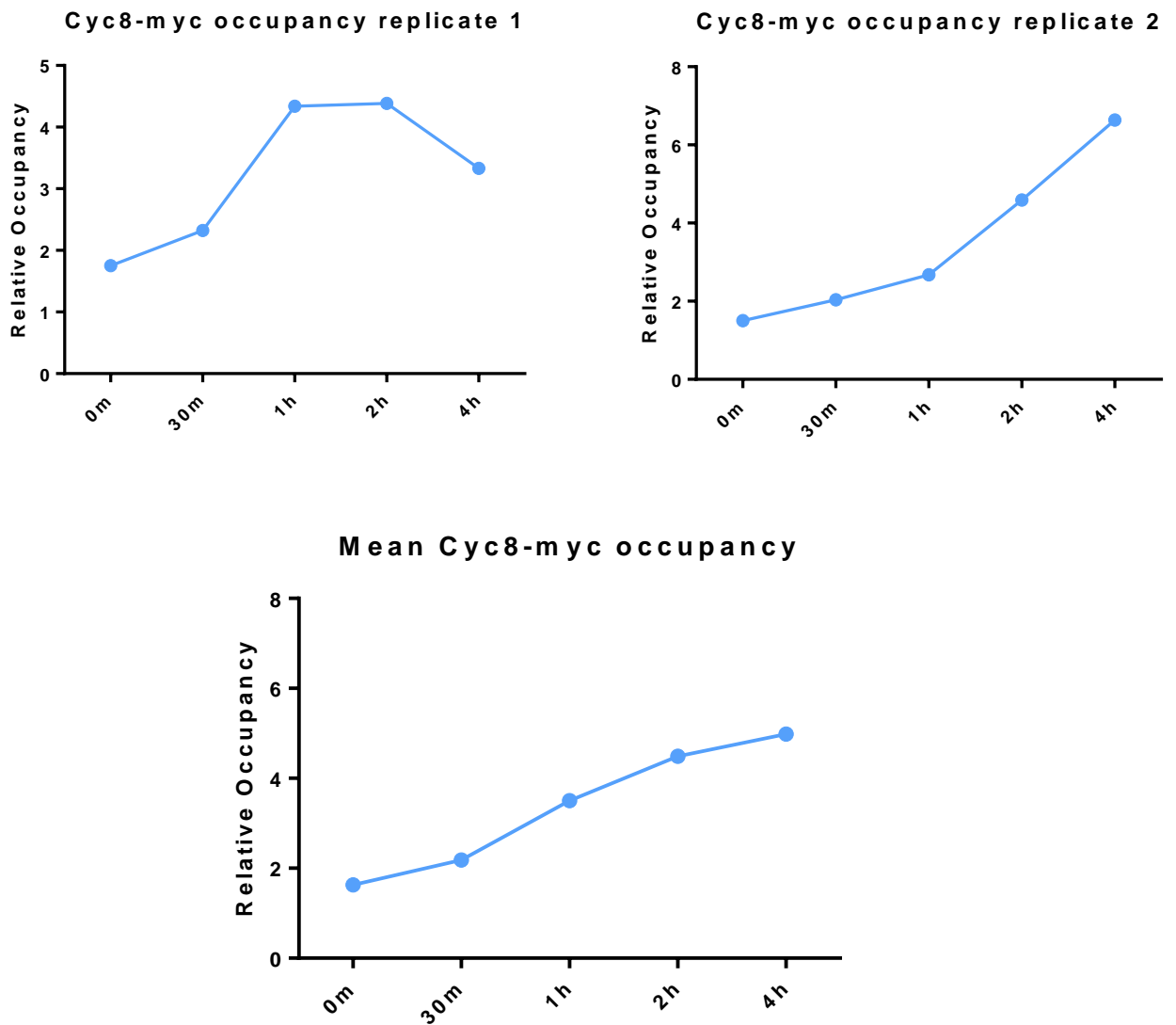


Figure 25. ChIP analysis of Cyc8-myc occupancy at the *FLO1* promoter. All occupancy levels are normalised to a telomeric control region (Tel V1). The plots shown are from each of the biological replicate experiments (replicates 1 - 2), and the mean value of the duplicate experiments.

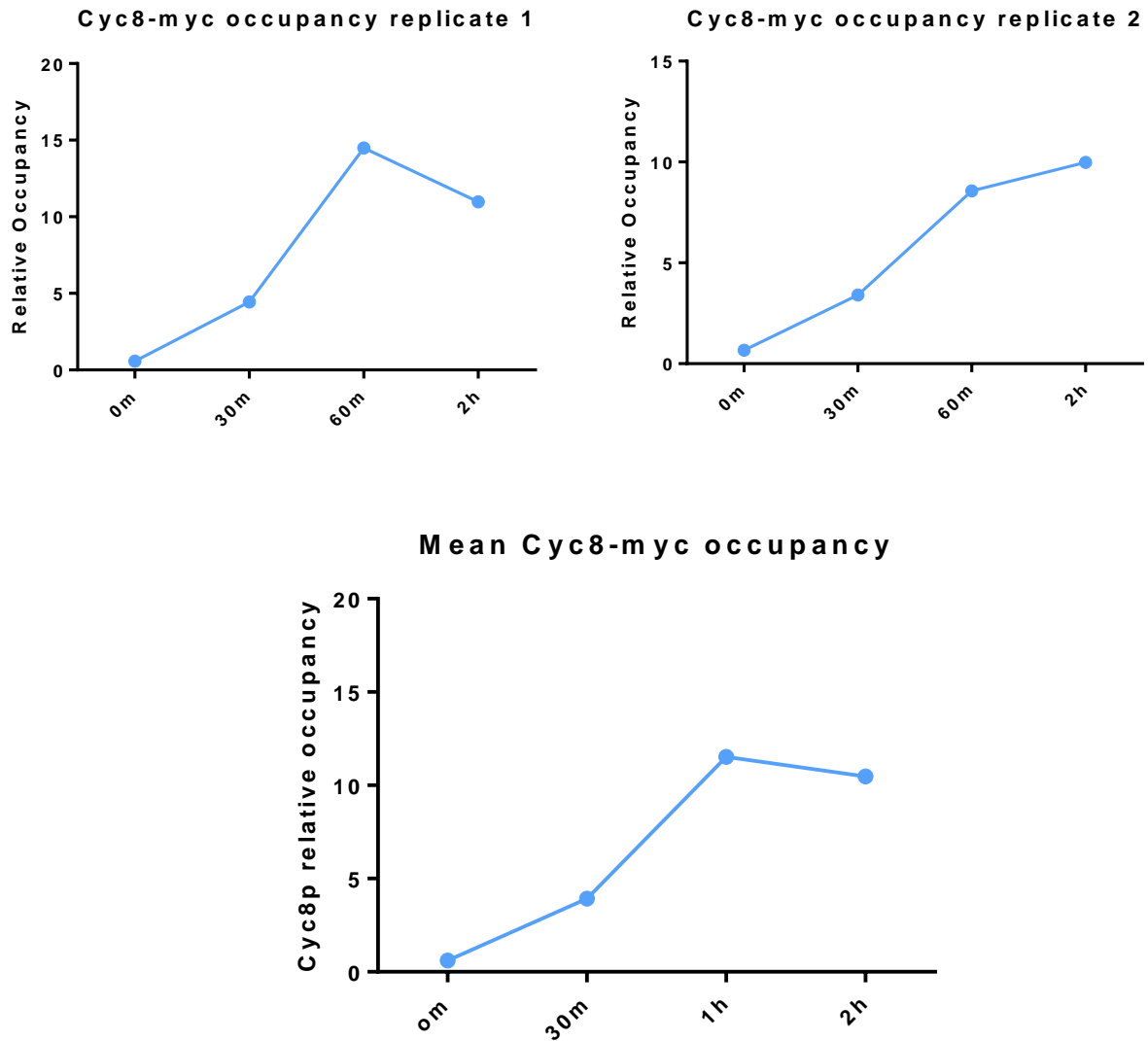


Figure 26. ChIP analysis of Cyc8-myc occupancy at the *SUC2* promoter. All occupancy levels are normalised to a telomeric control region (Tel V1). The plots shown are from each of the biological replicate experiments (replicates 1 - 2), and the mean value of the duplicate experiments.

6.10. Discussion

This analysis aimed at studying the occupancy of transcription regulating proteins at their binding sites in genes affected by Tup1-Cyc8, in a Tup1-AA time course, and comparing the results to data from a previous analysis in a Cyc8-AA time course.

The ChIP assay is a lengthy process and involves numerous steps. Hence, it was vital to optimize the protocol and test it. ChIP assay is an indirect measure of the protein levels and works on the assumption that only the segment of DNA closely bound to the protein of interest is precipitated.

Hence, correct fragment length of the sheared DNA is vital to the success of the experiment. Insufficient sonication results in longer DNA fragments, which may introduce false positive results. This means that the detected protein may be present much further away from the region of DNA targeted by the primer. Conversely, excessive sonication may result in shorter DNA fragments, which may introduce false negative results. Previous data from the Fleming lab suggested that 12 pulses of sonication of 10 seconds each at an amplitude of 8 microns were sufficient to shear the DNA to 100-500 bp fragments (Church 2015; Byrne 2020). These conditions were first tested on a WT sample and desired fragmentation was achieved. The fragment length was checked for each sample before processing it further (data not shown). These conditions worked consistently and did not have to be altered.

The first protein to be assayed was RNA Pol II. It is a good indicator of transcription levels. While the RNAPII levels at the *FLO1* ORF correlated well with the transcription and the sedimentation data, greater than background levels of RNAPII at time-zero was an interesting observation. This was consistent with previous observations in a Cyc8AA strain.

It suggests the existence of a greater than zero threshold level of RNAPII for the transcription of *FLO1*. However, this was not observed at the *SUC2* ORF, where the RNAPII levels at time zero were zero.

The next protein assayed was Tup1p. In genes derepressed in a Tup1AA time course, it was expected that Tup1 levels would be maximum at time zero and would decline with time. Indeed, this trend was observed in the *FLO1* promoter region. However, Tup1 was unexpectedly undetected at repressed *SUC2* (time-zero). This suggests that perhaps other factors present at the binding site may have rendered the Tup1 epitope inaccessible for binding with the ChIP antibody and thus, did not allow for its detection. Peak detection of Tup1 at 30 minutes following Tup1 depletion suggests that these factors are affected by the presence/abundance of Tup1 and are not masking it at this stage. The decline in Tup1 occupancy observed beyond 30 minutes following Tup1 depletion is most likely due to the Tup1 levels actually declining.

Next, Cyc8-myc levels were measured in the samples. At the *FLO1* promoter region, Cyc8-myc was detected throughout the time course, with its detection observed to increase with time. This suggests that the depletion of Tup1 from the Tup1-Cyc8 complex increases the availability of the Cyc8-myc epitope for binding with the ChIP antibody. Like Tup1, Cyc8-myc was also undetected at the repressed *SUC2*. It may be possible that the factors that are thought to mask the Tup1 epitope may also mask the Cyc8-myc epitope at the repressed *SUC2*. The increase in Cyc8-myc detection following Tup1 depletion is most likely an outcome of epitope unmasking, the same phenomenon that is likely at the *FLO1* promoter.

The anomalous observations regarding Tup1 and Cyc8-myc occupancy at the repressed *SUC2* promoter opens several possibilities in terms of candidates that may be masking the epitopes. The greater than background level detection of Tup1 at 30 minutes into the time-course despite the gene being derepressed suggests that complete depletion of Tup1 is not necessary for derepression. Observations of this nature could not have been made in a deletion strain, suggesting that the anchor-away strain is a superior model to study the functioning of the Tup1-Cyc8 complex.

It was reported that a mutant with a WD domain deletion, the domain which represses **a**-specific genes by binding to protein $\alpha 2$, had a greater derepressive effect on the **a**-specific gene *MFA2* than a *tup1* null. This suggests that the WD domain may constitute the repressor function while the Tup1 protein wholly may serve a dual function as a corepressor/coactivator (Parnell et al. 2021). Thus, it would be interesting to study the effect of anchor-away on the different domains of the complex in an attempt to uncover greater detail about the functioning and characteristics of the complex.

References

- Bookout AL, Cummins CL, Mangelsdorf DJ, et al (2006) High-Throughput Real-Time Quantitative Reverse Transcription PCR. *Curr Protoc Mol Biol* 73:15.8.1-15.8.28.
<https://doi.org/10.1002/0471142727.MB1508S73>
- Botstein D, Fink GR (2011) Yeast: An Experimental Organism for 21st Century Biology. *Genetics* 189:695–704. <https://doi.org/10.1534/GENETICS.111.130765>
- Boukaba A, Georgieva EI, Myers FA, et al (2004) A Short-range Gradient of Histone H3 Acetylation and Tup1p Redistribution at the Promoter of the *Saccharomyces cerevisiae* SUC2 Gene. *Journal of Biological Chemistry* 279:7678–7684.
<https://doi.org/10.1074/jbc.M310849200>
- Brown DT (2011) Histone H1 and the dynamic regulation of chromatin function.
<https://doi.org/10.1139/o03-049> 81:221–227. <https://doi.org/10.1139/O03-049>
- Byrne N (2020) Investigating the interplay between the Tup1-Cyc8 and Swi-Snf chromatin remodelling complexes in *Saccharomyces cerevisiae*
- Cavalieri V (2021) The expanding constellation of histone post-translational modifications in the epigenetic landscape. *Genes (Basel)* 12:.
<https://doi.org/10.3390/genes12101596>
- Church M (2015) Investigating regulation of gene transcription by the Tup1-Ssn6 co-repressor complex in *Saccharomyces cerevisiae*
- Church M, Smith KC, Alhussain MM, et al (2017) Sas3 and Ada2(Gcn5)-dependent histone H3 acetylation is required for transcription elongation at the de-repressed FLO1 gene. *Nucleic Acids Res* 45:4413–4430. <https://doi.org/10.1093/NAR/GKX028>

- Clapier CR, Iwasa J, Cairns BR, Peterson CL (2017a) Mechanisms of action and regulation of ATP-dependent chromatin-remodelling complexes. *Nature Reviews Molecular Cell Biology* 2017 18:7 18:407–422. <https://doi.org/10.1038/nrm.2017.26>
- Clapier CR, Iwasa J, Cairns BR, Peterson CL (2017b) Mechanisms of action and regulation of ATP-dependent chromatin-remodelling complexes. *Nature Reviews Molecular Cell Biology* 2017 18:7 18:407–422. <https://doi.org/10.1038/nrm.2017.26>
- Collart MA, Oliviero S (1993) Preparation of Yeast RNA. *Curr Protoc Mol Biol* 23:13.12.1-13.12.5. <https://doi.org/10.1002/0471142727.MB1312S23>
- Cooper GM (2000) *Chromosomes and Chromatin*
- Fleming AB, Beggs S, Church M, et al (2014) The yeast Cyc8–Tup1 complex cooperates with Hda1p and Rpd3p histone deacetylases to robustly repress transcription of the subtelomeric FLO1 gene. *Biochim Biophys Acta Gene Regul Mech* 1839:1242. <https://doi.org/10.1016/J.BBAGRM.2014.07.022>
- Fleming AB, Pennings S (2001) Antagonistic remodelling by Swi–Snf and Tup1–Ssn6 of an extensive chromatin region forms the background for FLO1 gene regulation. *EMBO J* 20:5219. <https://doi.org/10.1093/EMBOJ/20.18.5219>
- Gavin IM, Simpson RT (1997) Interplay of yeast global transcriptional regulators Ssn6p–Tup1p and Swi–Snf and their effect on chromatin structure. *EMBO J* 16:6263–6271
- Gillette TG, Hill JA (2015) Readers, writers and erasers: Chromatin as the Whiteboard of Heart Disease. *Circ Res* 116:1245. <https://doi.org/10.1161/CIRCRESAHA.116.303630>
- Govender P, Domingo JL, Bester MC, et al (2008) Controlled expression of the dominant flocculation genes FLO1, FLO5, and FLO11 in *Saccharomyces cerevisiae*. *Appl Environ Microbiol* 74:6041–6052. <https://doi.org/10.1128/AEM.00394->

08/ASSET/B5DF0FAC-E25F-4AAA-970F-

935563597A52/ASSETS/GRAPHIC/ZAM0190892370011.JPEG

Gromöller A, Lehming N (2000) Srb7p is a physical and physiological target of Tup1p.

EMBO J 19:6845. <https://doi.org/10.1093/EMBOJ/19.24.6845>

Haruki H, Nishikawa J, Laemmli UK (2008) The Anchor-Away Technique: Rapid,

Conditional Establishment of Yeast Mutant Phenotypes. *Mol Cell* 31:925–932.

<https://doi.org/10.1016/j.molcel.2008.07.020>

Hong L, Schroth GP, Matthews HR, et al (1993) Studies of the DNA binding properties of

histone H4 amino terminus. Thermal denaturation studies reveal that acetylation

markedly reduces the binding constant of the H4 “tail” to DNA. *Journal of Biological*

Chemistry 268:305–314. [https://doi.org/10.1016/S0021-9258\(18\)54150-8](https://doi.org/10.1016/S0021-9258(18)54150-8)

Jabet C, Sprague ER, VanDemark AP, Wolberger C (2000) Characterization of the N-

terminal Domain of the Yeast Transcriptional Repressor Tup1. *Journal of Biological*

Chemistry 275:9011–9018. <https://doi.org/10.1074/jbc.275.12.9011>

Jafri MA, Ansari SA, Alqahtani MH, Shay JW (2016) Roles of telomeres and telomerase

in cancer, and advances in telomerase-targeted therapies. *Genome Medicine* 2016 8:1

8:1–18. <https://doi.org/10.1186/S13073-016-0324-X>

Luo X-G, Guo S, Guo Y, Zhang C-L (2011) Histone Modification and Breast Cancer.

Breast Cancer - Focusing Tumor Microenvironment, Stem cells and Metastasis.

<https://doi.org/10.5772/24308>

Morrison AJ, Shen X (2009) Chromatin remodelling beyond transcription: the INO80 and

SWR1 complexes. *Nat Rev Mol Cell Biol* 10:373. <https://doi.org/10.1038/NRM2693>

Papamichos-Chronakis M, Conlan RS, Gounalaki N, et al (2000) Hrs1/Med3 Is a Cyc8-

Tup1 Corepressor Target in the RNA Polymerase II Holoenzyme. *Journal of*

Biological Chemistry 275:8397–8403. <https://doi.org/10.1074/JBC.275.12.8397>

- Parnell EJ, Parnell TJ, Stillman DJ (2021) Genetic analysis argues for a coactivator function for the *Saccharomyces cerevisiae* Tup1 corepressor. *Genetics* 219:.
<https://doi.org/10.1093/GENETICS/IYAB120>
- Pathan EK, Ghormade V, Deshpande M V. (2017) Selection of reference genes for quantitative real-time RT-PCR assays in different morphological forms of dimorphic zygomycetous fungus *Benjaminiella poitrasii*. *PLoS One* 12:e0179454.
<https://doi.org/10.1371/JOURNAL.PONE.0179454>
- Payankaulam S, Li LM, Arnosti DN (2010) Transcriptional repression: conserved and evolved features. *Curr Biol* 20:R764. <https://doi.org/10.1016/J.CUB.2010.06.037>
- Prakash K, Fournier D (2017) Histone Code and Higher-Order Chromatin Folding: A Hypothesis. *Genom Comput Biol* 3:41.
<https://doi.org/10.18547/gcb.2017.vol3.iss2.e41>
- Ramazi S, Allahverdi A, Zahiri J (2020) Evaluation of post-translational modifications in histone proteins: A review on histone modification defects in developmental and neurological disorders. *J Biosci* 45
- Rando OJ, Winston F (2012) Chromatin and Transcription in Yeast. *Genetics* 190:351.
<https://doi.org/10.1534/GENETICS.111.132266>
- Smith CL, Peterson CL (2004) ATP-Dependent Chromatin Remodeling. *Curr Top Dev Biol* 65:115–148. [https://doi.org/10.1016/S0070-2153\(04\)65004-6](https://doi.org/10.1016/S0070-2153(04)65004-6)
- Smukalla S, Caldara M, Pochet N, et al (2008) FLO1 is a variable green beard gene that drives biofilm-like cooperation in budding yeast. *Cell* 135:726.
<https://doi.org/10.1016/J.CELL.2008.09.037>
- Stratford M (1992) Yeast flocculation: A new perspective. *Adv Microb Physiol* 33:1–71.
[https://doi.org/10.1016/S0065-2911\(08\)60215-5](https://doi.org/10.1016/S0065-2911(08)60215-5)

- Szymanski EP, Kerscher O (2013) Budding yeast protein extraction and purification for the study of function, interactions, and post-translational modifications. *Journal of Visualized Experiments*. <https://doi.org/10.3791/50921>
- Teunissen AWRH, Van Den Berg JA, Yde Steensma H (1995) Transcriptional regulation of flocculation genes in *Saccharomyces cerevisiae*. *Yeast* 11:435–446.
<https://doi.org/10.1002/YEA.320110506>
- Tropberger P, Schneider R (2010) Going global: Novel histone modifications in the globular domain of H3. <https://doi.org/10.4161/epi.5.2.11075>
- Vallier LG, Carlson M (1991) New Snf Genes, Gal11 and Grr1 Affect Suc2 Expression in *Saccharomyces Cerevisiae*. *Genetics* 129:675.
<https://doi.org/10.1093/GENETICS/129.3.675>
- Varanasi US, Klis M, Mikesell PB, Trumbly RJ (1996) The Cyc8 (Ssn6)-Tup1 Corepressor Complex Is Composed of One Cyc8 and Four Tup1 Subunits. *Mol Cell Biol* 16:6707–6714
- Williams FE, Varanasi U, Trumbly RJ (1991) The CYC8 and TUPI Proteins Involved in Glucose Repression in *Saccharomyces cerevisiae* Are Associated in a Protein Complex. *Mol Cell Biol* 11:3307–3316
- Wong KH, Struhl K (2011) The Cyc8-Tup1 complex inhibits transcription primarily by masking the activation domain of the recruiting protein. *Genes Dev* 25:2525–2539.
<https://doi.org/10.1101/gad.179275.111>
- Yang L, Zheng C, Chen Y, Ying H (2018) FLO genes family and transcription factor MIG1 regulate *saccharomyces cerevisiae* biofilm formation during immobilized fermentation. *Front Microbiol* 9:1860.
<https://doi.org/10.3389/FMICB.2018.01860/BIBTEX>

Zemp I, Kutay U (2007) Nuclear export and cytoplasmic maturation of ribosomal subunits.

FEBS Lett 581:2783–2793. <https://doi.org/10.1016/J.FEBSLET.2007.05.013>

Zhang Z, Reese JC (2004) Ssn6–Tup1 requires the ISW2 complex to position

nucleosomes in *Saccharomyces cerevisiae*. EMBO J 23:2246.

<https://doi.org/10.1038/SJ.EMBOJ.7600227>